Pontifícia Universidade Católica
do Rio de Janeiro

Lua Selene da Silva Almeida

Mechanical Degradation of Polymer Solutions in Extensional Laminar Flow

Dissertação de Mestrado

Dissertation presented to the Programa de Pós-graduação em Engenharia Mecânica PUC-Rio in partial fulfillment of the requirements of the degree of Mestre em Engenharia Mecânica.

Advisor: Prof. Márcio da Silveira Carvalho

Rio de Janeiro
April 2021

Lua Selene da Silva Almeida

Mechanical Degradation of Polymer Solutions in Extensional Laminar Flow

Dissertation presented to the Programa de Pós-graduação em Engenharia Mecânica PUC-Rio in partial fulfillment of the requirements of the degree of Mestre em Engenharia Mecânica. Approved by the Examination Committee:

Prof. Márcio da Silveira Carvalho
Advisor
Departamento de Engenharia Mecânica – PUC-Rio

Profª. Mônica Feijó Naccache
Departamento de Engenharia Mecânica – PUC-Rio

Dr. Michel Ferreira Pinto
CENPES - Petrobras

Rio de Janeiro, April 19th 2021

Lua Selene da Silva Almeida

Bachelor in Aeronautics Civil Engineering, graduated from Instituto Tecnológico de Aeronáutica (ITA) in 2010.

Bibliographic data

Almeida, Lua Selene da Silva

Mechanical degradation of polymer solutions in extensional laminar flow / Lua Selene da Silva Almeida ; advisor: Márcio da Silveira Carvalho. – 2021.
59 f. : il. color. ; 30 cm

Dissertação (mestrado)–Pontifícia Universidade Católica do Rio de Janeiro, Departamento de Engenharia Mecânica, 2021.
Inclui bibliografia

1. Engenharia Mecânica - Teses. 2. PEO. 3. Polímero. 4. Degradação. 5. Capilar. 6. Microfluidica. I. Carvalho, Márcio da Silveira. II. Pontifícia Universidade Católica do Rio de Janeiro. Departamento de Engenharia Mecânica. III. Título.

CDD:621

To my beautiful Stella, for being the reason for it all.

Acknowledgements

This study was financed in part by the Coordenação de Aperfeiçoamento de Pessoal de Nível Superior - Brasil (CAPES) - Finance Code 001

To my parents, for paving the road and showing me the direction.

To my husband Eduardo for all the support, care and love.

To my advisor, professor Márcio Carvalho, for his support, trust and stimulus.

To my friend Letícia, for her support and inspiration.

To my friend Michel, for the patience.

To CNPq and PUC-Rio, for the aid granted, without which this work could not have been carried out.

Abstract

Almeida, Lua Selene da Silva; Carvalho, Márcio da Silveira (Advisor). **Mechanical Degradation of Polymer Solutions in Extensional Laminar Flow**. Rio de Janeiro, 2021. 59p. Dissertação de Mestrado - Departamento de Engenharia Mecânica, Pontifícia Universidade Católica do Rio de Janeiro.

Due to their physical-chemical behavior, water-soluble polymers are used extensively in various phases of drilling, completion, workover, and production of oil and gas wells. Therefore, it is fundamental to predict and to control in-situ porous medium behavior in order to understand polymer performance. Experiments were conducted to study the degradation of a semi diluted (2000 ppm) aqueous solution of PEO, using two capillaries with different entrance diameter (100 μm and 200 μm) both with 50 μm radius constriction, creating Fast-Transient Flows in their center. Different injection rates were imposed in order to observe different shear and extensional rates in the system. The effluent of the flow was collected, and reinjected, and rheological properties of the fluids were used as proxies for the degradation of the solution. We observed that for the more abrupt contraction, the minimum flow rate needed for degrading the polymer solution is lower. This result, when analyzed purely under shear rate perspective, is not reasonable, since the constriction shear rates to which the polymer is subjected are equal at both capillaries. Therefore, we inferred that the abruptness of the contraction plays a role in the degradation, which means elongational rate may be responsible for the lower critical flow rate. It was also observed a pattern for how the degradation occurs with subsequent injections. We could infer that subsequent injections cause incremental degradation before approaching a stabilization plateau and that higher flow rates generated lower degradation plateaus.

Keywords

PEO; polymer; degradation; capillary; microfluidic; extensional flow; IOR; FTF; polymer flooding

Resumo

Almeida, Lua Selene da Silva; Carvalho, Márcio da Silveira (Advisor). **Degradação Mecânica de Soluções Poliméricas em Fluxo Laminar Extensional**. Rio de Janeiro, 2021. 59p. Dissertação de Mestrado - Departamento de Engenharia Mecânica, Pontifícia Universidade Católica do Rio de Janeiro.

Devido ao seu comportamento físico-químico, os polímeros solúveis em água são utilizados em várias fases de perfuração, completação, e produção de poços de petróleo. Portanto, é fundamental prever e controlar o comportamento em meio poroso para entender o desempenho do polímero. Experimentos foram conduzidos para estudar a degradação de uma solução aquosa semi-diluída de PEO, usando dois capilares com diâmetros de entrada diferentes (100 μm e 200 μm) ambos com constrição de 50 μm, criando fluxos transientes rápidos em seu centro. Diferentes vazões foram impostas a fim de observar diferentes taxas de cisalhamento e de alongamento no sistema. O efluente do fluxo foi coletado e reinjetado, e suas propriedades reológicas foram utilizadas como proxies para a degradação. Observamos que, para a contração mais abrupta, a vazão mínima necessária para degradar a solução é menor. Este resultado, analisado apenas sob a perspectiva da taxa de cisalhamento, não é razoável, já que a taxa de cisalhamento na constrição a que o polímero é submetido é igual em ambos os capilares. Portanto, inferimos que a brusquidão da contração desempenha um papel na degradação, o que significa que a taxa de alongamento pode ser responsável pela menor taxa de fluxo crítico. Também foi observado um padrão de como ocorre a degradação com as injeções subsequentes. Podemos inferir que injeções subsequentes causam degradação incremental antes de se aproximar de um patamar de estabilização e que vazões mais altas geram patamares de degradação mais baixos.

Palavras-chave

PEO; polímero; degradação; capilar; microfluidica; fluxo extensional; EOR; FTF; injeção de polímero

Contents

List of Figures

List of Tables

An experiment is a question which science poses to Nature and a measurement is the recording of Nature's answer.

Max Planck

1
Introduction

1.1
The oilfield uses of Polymer Solutions

Due to their physical-chemical behavior, water-soluble polymers are used extensively in various phases of drilling, completion, workover, and production of oil and gas wells. For example, polymers can be used in drilling/completion fluids to provide the necessary viscosity profile and to control the loss of fluid to the rock formation. Once the well is producing, polymers can be used to control the oil/water ratio production, by forming crossed-link gel in situ and reducing the permeability of thief zones or high-permeability streaks. Water-based spacers can also exploit polymers to reduce friction pressure during well stimulation (Dong, et al., 2008). But its during water injection in mature fields that polymers can be used for long periods of time reaching extensive areas of the reservoir[1] in a large operation called: Polymer Flooding.

Waterflooding is one of the most widely known and implemented oil recovery processes worldwide. The injection of water displaces oil towards production wells via viscous, gravity, and capillary forces. Nevertheless, there are limitations for sweep efficiency of this secondary process[2] and much oil of the oil usually remains in the reservoir. Indeed, in some heterogeneous reservoir systems as much as 70% of the original oil may remain. (Sorbie, 2000). Thus, there is an enormous incentive for the development of improved or enhanced methods for recovering some portion

[1] The world's largest polymer flood was implemented at Daqing, in the Heilongjiang province of China, beginning in 1996. The first phase of the project lasted 12 years. By 2007, 22.3% of total production from the Daqing Oil Field was attributed to polymer flooding. Around 1 PV of polymer solution was injected for a given pattern, although a significant amount of variation and experimentation occurred to optimize performance. (Seright, 2017)

[2] Primary oil recovery describes the production of hydrocarbons under the natural driving mechanism – the compressional energy - in the reservoir without supplementary help from injected fluids such as gas or water. Secondary oil recovery refers to the introduction of some form of artificial drive in order to maintain reservoir pressure and also to sweep out oil in a more efficient displacement process.

of this remaining oil that is left behind either because it is trapped by the capillary forces or because it is in some way bypassed.

When the displacement is said to be inefficient, it is in the sense that there is early water production and low oil recovery at breakthrough. In order to understand how the introduction of polymer may enhance the sweep efficiency of the waterflood in the reservoir, it is necessary to introduce the concept of mobility ratio, M, defined as:

$$M = \frac{\lambda_o}{\lambda_w} = \frac{{\mu_o}/{k_o}}{{\mu_w}/{k_w}}$$

Where λ, μ and k are mobility, viscosity and effective permeability respectively and the subscripts *o* and *w* refer to oil and water.

In general, the inefficiency of the water-oil displacement mechanism is a result of either an unfavorable mobility ratio or large-scale heterogeneities in the reservoir, like stratification or channeling. In a displacement process, a mobility ratio that is greater than 1 is considered unfavorable, while a mobility ratio that is less than 1 is considered favorable.

Addition of polymer increases the viscosity of its aqueous phase and decreases the permeability to water so that the mobility of aqueous phase decreases. Thus, the decrease in mobility ratio improves the displacement efficiency and increases the volume of reservoir that is contacted by the injection fluid. This can delay the flood breakthrough to the production well while also producing oil at a higher rate. Polymer flooding has considerably higher oil recovery potentials than waterflooding—typically on the order of 6%–12% higher, which gives a 40%–50% recovery factor of initial oil in place (IOIP) after application. (Speight, 2019)

When polymers are used in oil recovery operations, it is clearly important that the polymer properties are not rapidly degraded. The degradation process essentially breaks the large molecules into smaller ones, affecting the molecular weight distribution of the polymer and consequently its rheological properties and flow characteristics. For oil recovery applications, the main types of degradation can be

classified by their cause (i) chemical – through processes like oxidation or hydrolysis, (ii) mechanical – as result of high mechanical stresses on the macromolecule and (iii) biological – through microbial breakdown of the polymer chain.

Roughly there are two types of polymers that can be used for improving the oil recovery in the reservoir: synthetic polymers (such as polyacrylamides) and biopolymers (such as xanthan). Typical examples of synthetic polymers are polyacrylamides and its derivatives such as partially hydrolysed polyacrylamide (HPAM), hydrophobically associating polyacrylamide (HAPAM), and copolymers of acrylamide. On the other hand, biopolymers include xanthan gum, scleroglucan, hydroxyethylcellulose, carboxymethylcellulose, welan gum, guar gum, schizophyllan, cellulose, and lignin.

Synthetic partially hydrolyzed polyacrylamides (HPAM) are the most widely used polymers in polymer flooding. Generally, the degree of hydrolysis is between 25-30% (van den Ende, 2015). Compared to biopolymers such as xanthan, HPAM are more prone to mechanical degradation. This process is usually very intense in the high flow rate region close to the well-bore, and although it has frequently been referred to as 'shear degradation' in the literature, the term is not strictly correct. (Sorbie, 2000) This behavior is attributed to the conformation of the macromolecules. While Xanthan molecule structure can be considered as a rigid rod that will align in the direction of the flow, HPAM is a flexible chain with a coiled conformation that can be stretched by the flow (Jouenne, et al., 2018).

1.2 General concepts

One of the most important property of a polymer solution for oilfield use is its viscosity. Therefore, it is fundamental to predict and to control the polymer solutions viscosity in porous medium behavior in order to understand polymer flooding performance. In laying out the problem, it is necessary to introduce a few concepts.

1.2.1
Laminar x Turbulent regime

In laminar flow, named from the Latin *lāmina*, meaning layered, lines of flow remain parallel, and mixing does not occur. Conceptually, laminar flow occurs when viscous forces are higher than inertial forces. Hence, in highly viscous fluids, laminar flow can be demonstrated with relative ease, while in fluids with very low viscosity (water, most gases, etc.), it may be difficult to establish fully laminar flow. (Ramsey, 2019). On the other hand, fully developed turbulent flow is characterized by vigorous mixing across the entire cross-sectional area of the flow.

The occurrence of turbulent flow is related to the Reynolds number defined as:

$$Re = \frac{VD\rho}{\mu},$$

Where D is the diameter of the flow channel, in ft or m, V is the average velocity of the fluid in the channel, and μ is the viscosity of the fluid of Newtonian fluid or effective viscosity of non-Newtonian at the flow condition.

The Reynolds number is the ratio of inertial forces to viscous forces. It is a dimensionless number used to categorize flows with respect to the relative importance of inertial and viscous forces.

The flow regime is typically divided in three cases on the basis of the value of the Reynolds number. In the flow through a circular tube, for Re<2000 the flow is laminar; for Re>3000 the flow is turbulent, while for 200<Re<3000 the flow falls in an intermediate regime. However, recent experiments (Chandra, et al., 2018) have shown that the addition of polymer, at sufficiently high concentrations, destabilizes the flow when compared to that of a Newtonian fluid, thereby providing evidence for ‘early transition’ or ‘elasto-inertial turbulence’ in the flow of polymer solutions.

1.2.2
Rheological behavior of polymer solutions under different types of flow

Some polymer macromolecules are flexible chains. In the absence of flow, or in sufficiently weak flows, they are in a coiled state and act hydrodynamically as spheres. When it comes to a moving fluid though, the dynamics of a flexible polymer depends strongly on the properties of the velocity gradients, or the type of flow.

Simple shear flow, also known as Couette flow, it is characterized by a constant shear stress distribution and may be represented as a superposition of a purely rotational flow and a purely elongational flow, as schematized in **Figure 1.** Considering a fluid element of the solution in such flow, both the elongational and rotational components of the strain rate are equal. The presence of a differential velocity across the flow field encourages the molecule to rotate, reducing the stretching induced in the molecular chain. In other words, before the chain is greatly extended it has rotated into a position in which the flow is reversing that extension. Therefore, full extension and/or alignment is not achieved. In fact, in the case of flexible chains the coil will only be slightly deformed.

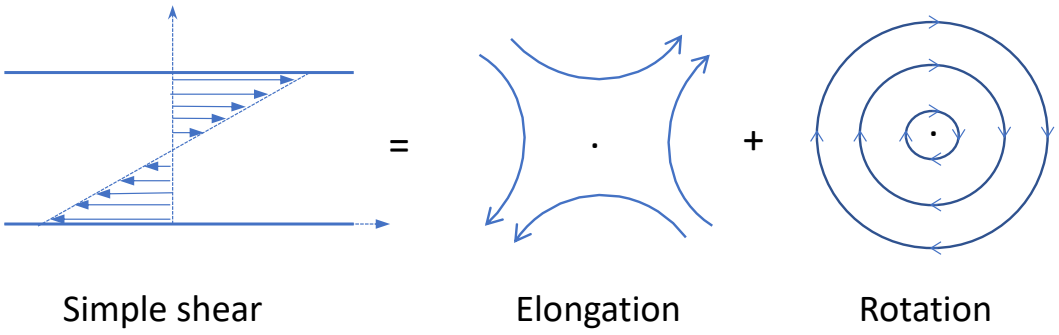

Figure 1- Schematic illustration of the streamline in a simple shear, represented as a superposition of a purely rotational flow and a purely elongational flow.

In simple shear flow, the vast majority of dilute polymer solutions[3] are pseudoplastic, or shear thinning. More specifically, such polymer solutions typically show Newtonian behavior at sufficiently low flow rate, followed by a

[3] According to (Sorbie, 2000), this characteristic is found in Improved Oil Recovery (IOR) polymers.

region of shear thinning where the viscosity of the fluid decreases. A common way to plot this simple rheological behavior is as viscosity against shear rate, as depicted in **Figure 2.**

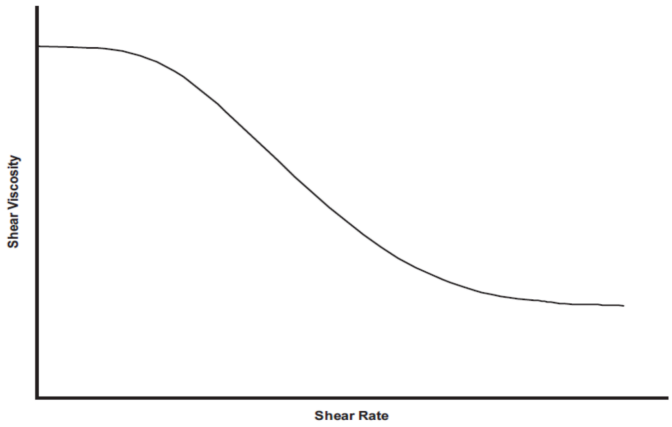

Figure 2 - Schematic of the shear-thinning behavior of polymer solutions on log-log scales (van den Ende, 2015)

Although most rheological studies are carried out in simple shear flows such as those found in rotational viscometers, real flows experienced by real liquids often have extensional nature, and for some liquids there can be a very large difference between their shear and extensional viscosities.

Extensional flow is characterized by a direction along which the fluid element is in a continuing state of extension. Pure extensional flow does not involve shearing and is sometimes referred to as "shear-free" flow. In this situation, the preferred orientation of the molecules is in the direction of the flow because there are no competing forces to cause rotation, they can elongate drastically and even break. This is the reason why mechanical degradation of polymer solutions is mainly studied through extensional flows.

In the same way that there is a stress and a deformation rate in shear flow, there is the extensional stress, σ_e and the extension rate, $\dot{\varepsilon}$. The ratio of the stress and rate gives the uniaxial extensional viscosity $\eta = \sigma_e/\dot{\varepsilon}$.

According to (Keller & Odell, 1985), when placed in such flow, a flexible chain should respond to an increase in extensional rate from an almost random state to

practically full extension at a critical rate value $\dot{\varepsilon}_c$. In other words, a polymer molecule will uncoil in a coil-to-stretch transition provided the extensional rate exceeds the slowest molecular relaxation rate.

This coil-stretch transition results in a great increase in extensional resistance, to give a viscosity that can be up to thousands of times higher than the equivalent viscosity in shear flow, as illustrated in **Figure 3** and **Figure 4.**

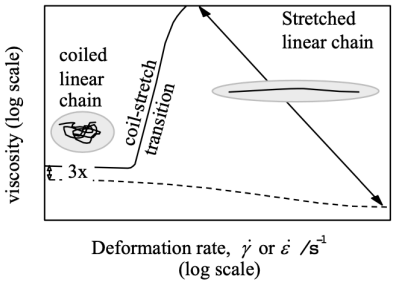

Figure 3 - The shear (dotted line) and extensional (solid line) viscosities of a dilute solution of linear polymer, showing the coil stretch transition from coiled to unwound configuration. (Barnes, 2000)

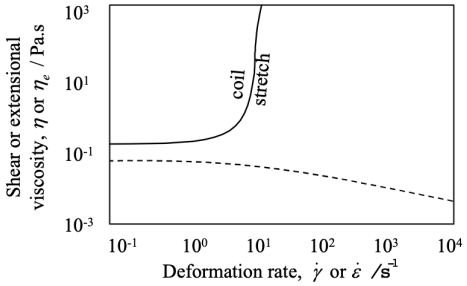

Figure 4 - The shear (dotted line) and extensional (solid line) viscosities of an aviation fuel with an anti-misting agent added.

This initial resistance to elongation can be characterized by the conformational relaxation time (τ) appropriate to the random coil given by:

$$\tau = \frac{1}{\dot{\varepsilon}_c}$$

The relaxation time is related to the amount of elastic energy being stored by the fluid and it is a key parameter for characterizing a viscoelastic fluid.

Viscoelastic fluid shows both elastic and viscous characteristics under certain conditions, with the ability to store and dissipate energy when the fluid molecule is subjected to deformation. In contrast, Newtonian fluids are purely viscous, and their relaxation time is zero.

There is not really an agreement in literature about the flow rate at which the elastic effect becomes dominant. However, it is agreed that they become important when

the fluid is significantly deformed in a time comparable to the relaxation time[4] of the fluid. (van den Ende, 2015)

In other words, the onset of viscoelastic effects occurs at velocities in which the time to pass one pore is in the same order of magnitude as the polymer time constant. If the velocity is further increased the polymer is degraded because of rupture of the polymer chain. (Stavland, et al., 2010) As the chain starts to extend, hydrodynamic forces exerted through the friction of the solvent on the stretched chain are increased and can lead to chain rupture. The chain is totally stretched if the residence time in the elongational field is sufficient. (Jouenne, et al., 2018)

To observe the uncoiling of the molecular chains, it is necessary an experimental apparatus in which the fluid element is submitted to both an elongational shear stress that is sufficiently high and a residence time that is long enough for the macromolecule to stretch. Two kinds of extensional devices are reported in the literature: devices with a stagnation point and devices with an abrupt contraction. Such devices enable extensional flow under Quasi-Steady State and Fast Transient State respectively. (Dupas et al., 2012)

1.2.3 Porous media flow

Due to tortuosity of porous media and existence of several contraction-expansion channels, polymer solutions will be exposed to a wide range of shear rates at each flow rate, resulting in a significantly complex rheology behavior. (Skauge, et al., 2018)

Moreover, extensive experimental results (Dauben & Menzie, 1967) (Smith, 1970) (Seright, 1983) (Seright et al., 2010) (Al-Shakry et al., 2018) have shown decreased mobility for different polymers in porous media. Although there are different mechanisms involved, like polymer-matrix interactions and solution rheology, the mobility decreases do not correlate with adsorption of the polymers. Viscoelastic behavior, however, provides a basis for a convenient measure of the mobility

[4] The relaxation time is affected by the nature of the frictional contact between molecule and solvent which depends on molecular shape, solute-solvent interaction and solvent viscosity. (Keller & Odell, 1985)

control activity of some polymers: increased flow resistance results from rapid flow through expansions and contractions (Jennings et al., 1971).

Therefore, when a polymer with elastic properties is flooded through a porous medium, there are different rheological regimes that can be observed. At low to moderate flow rates, the apparent polymer viscosity is shear thinning, a shear dominant flow regime. However, at higher flow rates, the viscosity increases by increasing the shear rate, an extensional dominant flow regime. Which means that not only the polymer viscosity varies with shear rate, but also the way it varies is affected by the shear rate itself. This behavior is illustrated in **Figure 5** and can be explained by viscoelastic effects and elongation of the polymer inside the pore structure (Stavland, et al., 2010).

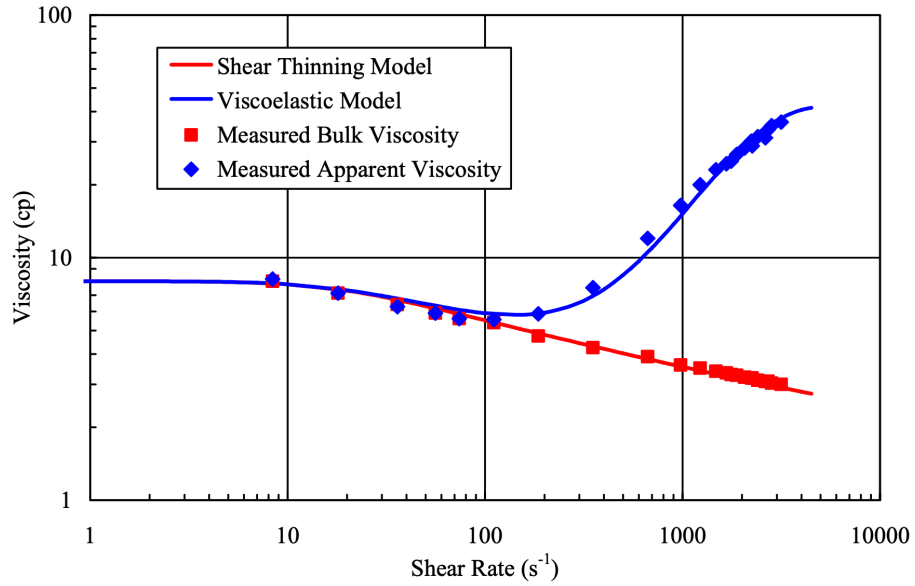

Figure 5 – Measured bulk viscosity and measured apparent viscosity (in porous media) respectively compared to the shear thinning model – Carreau model – and to the viscoelastic model proposed by the author. (Delshad, et al., 2008)

The measured apparent viscosity presented in the blue curve for the coreflood is calculated with the help of Darcy's Law, as:

$$\mu_{app} = \frac{kA\Delta P}{qL},$$

Where k is permeability, A is the cross-sectional area of the core, q is the flow rate and L is the length of the core.

The effective shear rate in the core is given by:

$$\gamma = C\left[\frac{3n+1}{4n}\right]^{n/(n-1)}\left[\frac{u_w}{\sqrt{k_w S_w \emptyset}}\right],$$

Where n is a polymer-specific constant; u_w is Darcy velocity of the polymer-containing water phase; k_w is the water permeability; S_w is water saturation and $\emptyset$ is porosity; C in general is a function of permeability and porosity, but according to (Delshad, et al., 2008), C = 6 fits a variety of coreflood data.

Although it is not in the scope of this study, it is worth it to mention that there are increasing laboratory and field evidence that the viscoelastic characteristics of polymer solutions can help improve polymer-flood efficiency. Simply put, the presence of a shear-thickening fluid for the bulk of the reservoir volume is more effective in displacing the bypassed oil from the low-permeability zone. (Delshad, et al., 2008)

1.2.4 Extensional viscosity measurements

In order to study different extensional flow, there are several types of devices detailed in literature. However, there is one recurring problem with common extensional measurements: it is difficult to be sure if steady state has been achieved. In simple rotational shear instruments, the attainment of steady state is just a matter of waiting. In extensional instruments though the amount of deformation is usually small compared with that necessary to reach equilibrium, which for some polymeric systems can sometimes only be reached at over 1000 times extension of the undeformed sample at its rest state. (Barnes, 2000)

In this section, we describe how Quasi-Steady State Flow and Fast Transient Flow devices are designed and how macromolecules flow through each of them.

Quasi-Steady State Flow (QSSF)

The QSSF devices are designed to trap some fluid elements within the flow-field due to the presence of a stagnation point. The region surrounding such point provides long residence times for the streamlines that pass close to it, so that steady-

state molecular conformations can be achieved, and quasi-steady-state flow is established.

In the vicinity of the stagnation point some fluid elements remain trapped within the flow-field over a long period of time. The macromolecules contained by such fluid elements can be subject to strain rates large enough for flexible coils to extend.

As proposed by (Frank, et al., 1971), a way of achieving a large strain rate free from rotation is to let two opposed fluid jets meet as shown in **Figure 6.**

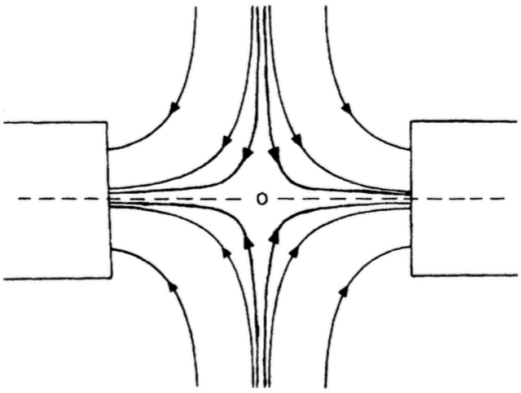

Figure 6 - A schematic view of the opposed jets and the flow-field created between them (Nguyen & Kausch, 1999)

The system consists of two cylindrical jets facing each other and immersed in a polymer solution. On the axis and the plane of symmetry and its vicinities, high strain rates occur, and the rotation rate is zero. There is a point of zero velocity at the center of symmetry of the system – denoted "o" in **Figure 6** – so that the time of injection for an axial fluid element becomes in principle infinite. (Frank, et al., 1971). The same considerations apply if the fluid is either blown out or sucked through both jets.

The flow in the liquid between the jets contains a high degree of extensional flow, and by noting the jet orifice size and the flow rate as well as the reaction on one of the jets, then a measure of the extensional viscosity can be obtained (Barnes, 2000).

Moreover, the cross-slot device and the "four-roll mill" can also be used to create a QSSF for elongational flow studies. A schematic view of the cross-slot device

used to create a planar extensional flow by (Miles & Keller, 1980) and the idealized flow field in the cross-slot are depicted by **Figure 7** (a) and (b) respectively. The arrows indicate the fluid direction. The exact center is the locality of zero velocity, i.e. stagnation *line* – since the flow is planar.

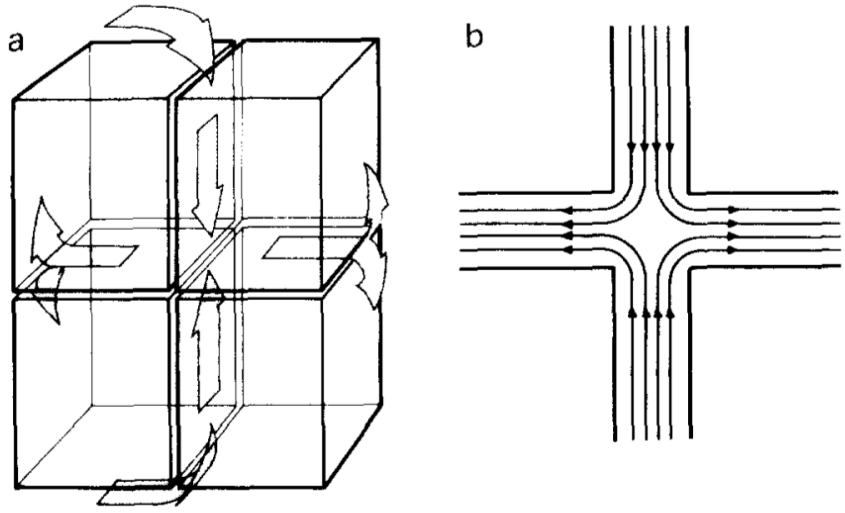

Figure 7 - (a) Cross-slot device used to produce a planar elongational flow field; (b) idealized flow field in the cross-slot (Miles & Keller, 1980)

The 'four-roll mill' is a device invented in the 1930s for studies of drop deformation and burst in two-dimensional, pure extensional flows. This device produces a very good approximation to a linear flow in the region between the four rollers, and it allows the magnitude of the rate-of-strain tensor to be arbitrarily selected by various combinations of roller speed and direction. Furthermore, there is a stagnation point located centrally between the rollers as observed in **Figure 8.** Thus, in principle, the particle or drop of interest will remain at a fixed position in the device, even if the flow is time-dependent[5]. (Bentley & Leal, 1986)

[5] Unsteady flow or transient.

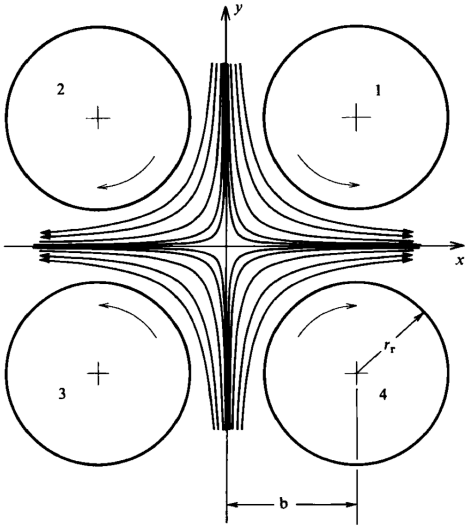

Figure 8 - A schematic view along the rollers of four-roll mill device. The stagnation point is located in the origin of the axis x and y.

a) Fast Transient Flow (FTF)

FTF devices are characterized by the presence of an abrupt contraction (or divergence) that generates a sudden acceleration of the polymer solution. In this type of flow, the residence time is often smaller than the polymer relaxation time and mechanical degradation may occur even though macromolecules are only partially extended. (Dupas et al., 2012)

(Ryskin, 1987) postulates a 'coil-string-coil' configuration of the macromolecule during the transient process of the supercritical stretching. The central portion 'string' is straightened out first and then remains taut and grows in length at the expense of the two coiled portions at the ends. If the flow later becomes weak, the chain will curl back into a coil. In other words, each half of the chain unravels (in a strong flow) and curls back (in a weak flow) just like the string in a 'yo-yo'.

According to (Rabin, 1988), in QSSF the equation that expresses the critical strain-rate for the molecule fracture depends only on the molecular weight of the polymer. On the other hand, in FTF, it depends on the quality of solvent. Also, the distribution of fracture products should be broader for FTF than for QSSF, and there is a possibility of observing non-central scission in the former case.

1.2.5
Semi-dilute solution

The discussion presented so far of the stretching and breaking of polymers has been based on experimental and theoretical studies of polymers in dilute solutions subjected to elongational flows.

As the solution concentration is increased from the dilute regime, there are more relevant interactions between chains, thus it is expected a dramatic effect on viscosity and viscoelastic properties. The increasing extensional viscosity will perturb the flow field and, ultimately, the polymer chains would begin to overlap and behave as an entangled network. (Nguyen & Kausch, 1999)

Above this entanglement concentration (c^*), a given chain feels an extra stress resulting from the hydrodynamic interactions with the surrounding other chains, thus should break more easily in the same macroscopic flow field. (Nghe, et al., 2010)

1.3
Objective of research

The objective of this research is to study the mechanical degradation of aqueous polymer solution subjected to extensional flow, by putting into practice the theories of porous media flow of complex rheology fluids combined with macromolecule concepts.

With this objective in mind, the specific aim of the work is to conduct experimental investigation of the polymer degradation using Fast Transient Flow devices and to characterize the effluents rheology properties.

2
Methodology and materials

Experiments were conducted to study the degradation of polymer solutions, using a microfluidics system which creates a Fast-Transient Flow in its center. Different injection rates were imposed in order to observe different shear and extensional rates in the system. The effluent of the flow was collected, and rheological properties of the fluid were used as proxies for the degradation of the solution. As expected for microfluidics system, the experiment was conducted in the laminar flow regime for all the flow rates imposed.

2.1
Poly (ethylene oxide) - PEO

The polymer solutions used in this study are semi-diluted aqueous solutions of poly (ethylene oxide). PEO is one of the most extensively studied of all water-soluble synthetic polymers, both for its wide range of applications and from the fundamental standpoint of understanding the behavior of polymer solutions. It is a flexible non-ionic polymer and, according to (Devanand & Selser, 1990), in carefully purified water, its molecules behave like a typical random coil.

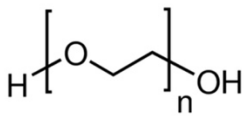

Figure 9 – Molecular structure of PEO

The solutions were prepared with Sigma Aldrich PEO powder with an average molecular weigh $M_V \sim 8.000.000$ shown in **Figure 10.**

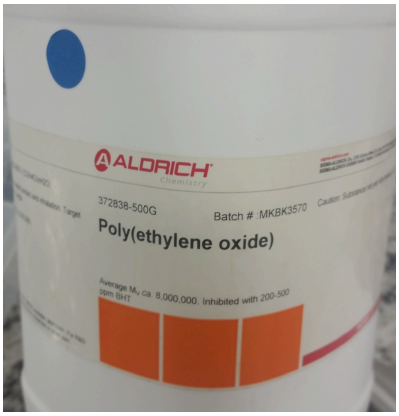

Figure 10 – Polymer powder used in the experiments

To prepare the solution, deionized water and polymer powder are weighted and then mixed by the mechanical stirrer Eurostar digital IKA Werke, shown in **Figure 11.**

Figure 11 – Preparation of the polymer solution

In general, a master (stock) solution is made, from which other solutions are diluted and tested. For this study, the master solutions were prepared in 500 g batches at a polymer concentration (C) of 5000 ppm.

The polymer concentration, in parts per million, for both dilute and master solutions, is calculated using a simple equation:

$$C\ (ppm) = \frac{mass_{polymer}}{\left(mass_{water} + mass_{polymer}\right)} * 10^6$$

The master solutions were covered, sealed, and allowed to hydrate for approximately 12 hours before use.

2.2
Experimental Apparatus

2.2.1
Capillaries

To study the mechanical elongational degradation of the polymer solution, fast transient flow was created in the abrupt contractions of capillaries, as schematized in

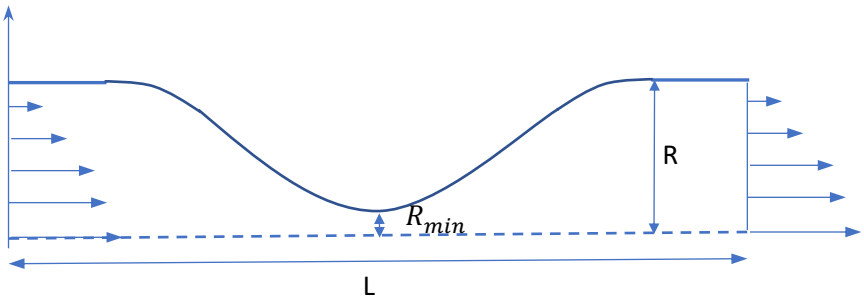

Figure 12.

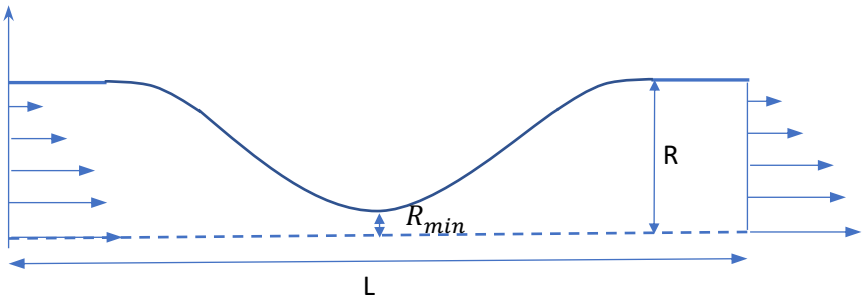

Figure 12 – Schematic representation of the geometry of abrup contractions used to create extensional flow

To create different strain rates for each flow rate, capillaries with two different entrance diameters, D, were used, resulting in two D: D_{min} contractions: 200:50 and 100:50, where $R_{min} = D_{min}\ /2$ is the throat radius.

Figure 13 and

Figure *14* are images of both capillaries, obtained by Zeiss AxioCam MRC5 7820.

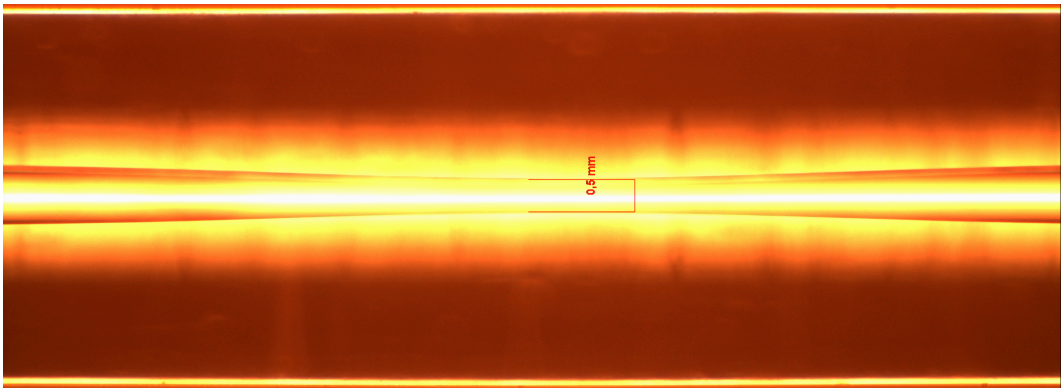

Figure 13 – Microscopic image of the capillary 100:50 showing the 50 µm constriction

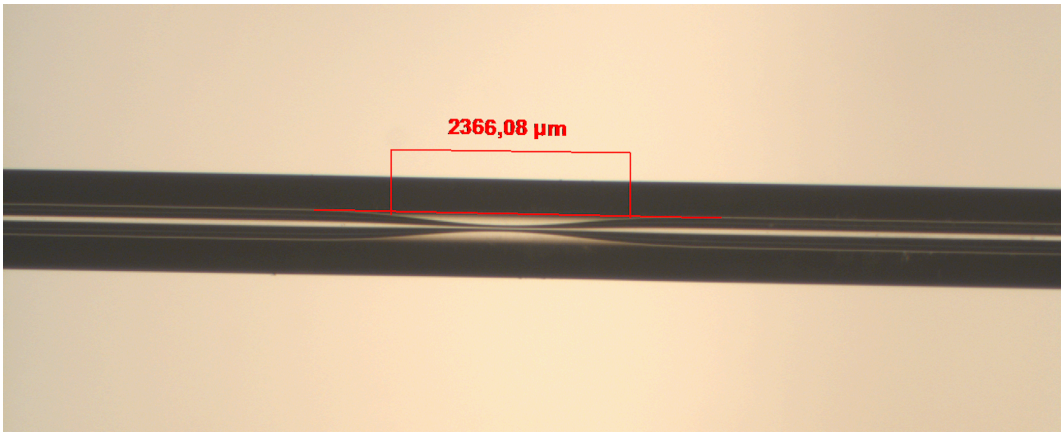

Figure 14 - Microscopic image of the capillary 200:50

2.2.2 HPLC JASCO PU 2086i

The polymer solutions were injected into the capillaries by a dual-piston chromatography pump (Jasco PU 2086i), illustrated by **Figure 15.**

According to the manufacturer, the dual plunger design eliminates pulsation providing uniform flow with flow rate precision of less than 0.2%.

Figure 15 - HPLC pump JASCO PU 2086i

Even though considerable mechanical degradation is not expected from using a piston pump, effluent was collected at the exit of the pump at each analyzed flow rate to be the method blank, the basis for comparison of the capillaries effluents. This way, any possible degradation due to the pump is not misinterpreted as capillary degradation.

2.2.3 Rheometer

The rheological properties of the PEO solutions were measured using the Thermo Scientific™ HAAKE™ MARS™ 3 rheometer, illustrated by **Figure 16.** The concentric cylinder, double-gap geometry, was chosen due to its lower inertia and higher sensitivity. Dynamic viscosity curves in the range of shear rates from 1 to 1000 s^{-1} at a constant temperature of 298.15 K were determined.

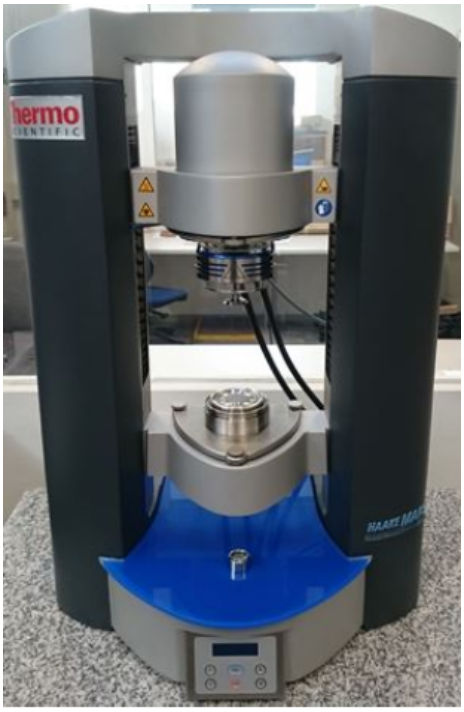

Figure 16 - HAAKE MARS III rheometer

2.2.3.1 Limitations of the rheometer measurements

Although rheometers have a large usage in the oil industry for characterizing a myriad of fluids flown by the reservoir, there are a number of limitations to their measurements to be taken in consideration when interpreting the experimental results.

The theoretical definitions of material functions are based on stress, strain, and strain-rate components in simple deformation fields, but experimental techniques measure displacements and loads, such as forces or torques.

Therefore, in order to obtain the rheology properties of complex fluids, which are defined from deformations in terms of strain and stress, assumptions are required. Displacement needs to be converted to strain and similarly, load to stress. Therein lies the risk that non-ideal conditions exist as shown in **Figure 17.**

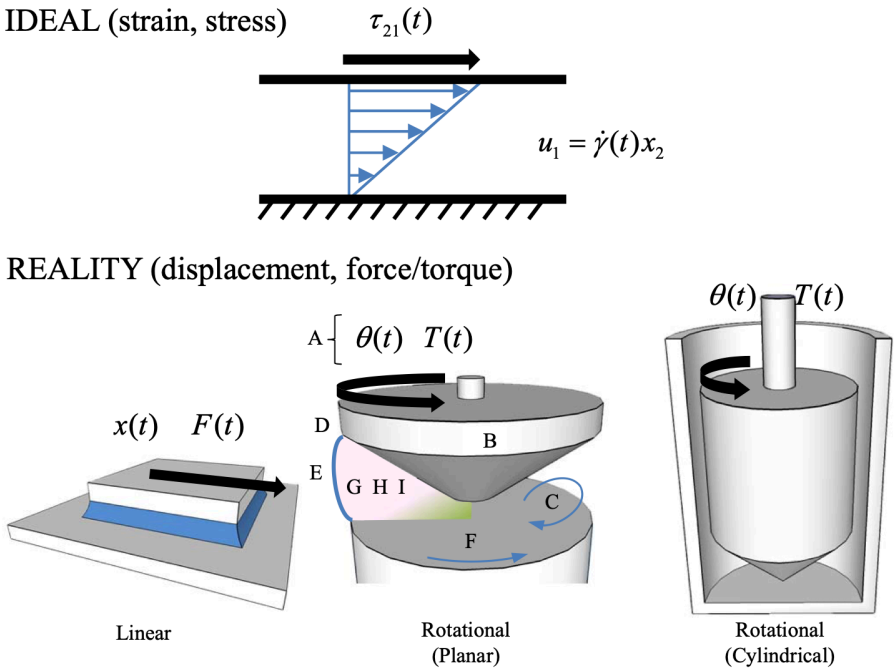

Figure 17 - Ideally, shear rheological properties are defined from strain γ(t) and stress τyx(t) in homogeneous simple shear. In reality, boundary displacements and loads are measured, and non-ideal experimental artifacts must be considered. (Ewoldt & Caretta, 2015)

The minimum torque is typically the most important limitation for the rheometer measurements of the polymer solution. Minimum torque is specified by instrument manufacturers but can often be higher due to a myriad of experimental challenges. (Ewoldt & Caretta, 2015)

Consequently, the effects of the experimental challenges when entering the small torque range at low shear rates, such as the typical increase of experimental scatter, are well reported in literature (Pinho et al., 2011) (Johnston & Ewoldt, 2013) (Dijkstra et al., 2014).

The data collected for this work also shows data scattering and torque deviations at low shear rates. Next section describes the model used to mitigate such errors when interpreting the viscosity curves obtained[6].

[6] The outliers from the data collected as well as great deviations from the shear thinning behavior were not considered in the model fit.

2.3
Carreau Model

Aqueous solutions of IOR polymers are generally pseudoplastic, and the most common way to plot this rheological behavior is as viscosity against shear rate, as shown in **Figure 2.** Such polymer solutions typically show Newtonian behavior at sufficiently low flow rate, followed by a region of shear thinning where the viscosity of the fluid decreases. At very high shear rates, the tendency is for the viscosity to approach a second plateau value just above the solvent viscosity.[7]

As discussed in the previous section, there are limitations of the rheometer measurements conducted, which can bring difficulties to the interpretation of results.

When working with macromolecular fluids, it is important to characterize material properties and a model can be useful for an estimation of viscosity beyond what might be capable to be measured with available tools.

A satisfactory model for shear thinning fluids is the Carreau equation, a type of generalized Newtonian fluid model where the viscosity depends upon the shear rate by the following equation:

$$\frac{\eta - \eta_\infty}{\eta_0 - \eta_\infty} = (1 + (\lambda\gamma)^2)^{\frac{n-1}{2}}$$

Where η_0 is the zero-shear rate viscosity, η_∞, the infinite shear rate viscosity, λ, a time constant and n is a dimensionless constant, typically in range $0.4 \leq n \leq 1.0$ for pseudoplastic fluids.

Although data was obtained in the range of shear rates from 1 to 1000 s^{-1}, it was observed data scattering and torque deviations at low shear rates (between 1 and 10 s^{-1}), as discussed in the previous section. Therefore, part of the data was not considered for obtaining the model parameters and is not shown in the graphs of

[7] As discussed in Section 1.2.5, the second plateau is not observed in porous media flow apparent viscosity.

this study. **Figure 18** exemplifies the typical curve obtained by using the Carreau equation for the viscosity data.

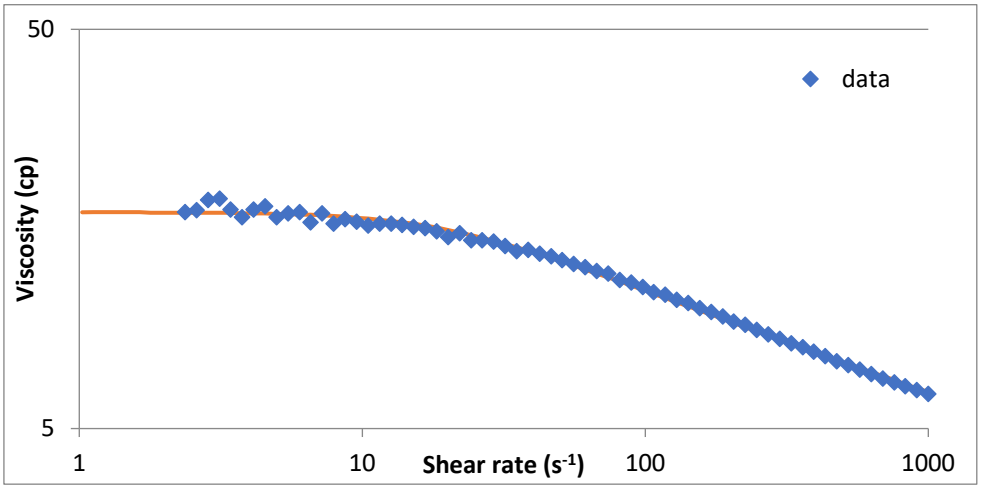

Figure 18 – Typical curve obtained in this work scope by using the Carreau equation for the viscosity data of PEO 2000 ppm.

2.4 Experiment description

A semi diluted (2000 ppm) aqueous solution of PEO was injected into both capillaries. For each injection, the effluent was collected and separated in two: 7 ml was subjected to rheometer measurement and the rest of the effluent was reinjected into the capillary. This procedure was repeated at least until the fourth injection of the solution through the capillary for different flow rates[8].

The data collected from the rheometer was adjusted into the Carreau Model so as to obtain the first Newtonian plateau viscosity, or zero shear viscosity. The degradation of the solution was then obtained by comparing each effluent zero shear viscosity, η_0 , with the initial solution shear viscosity, ${\eta_0}^i$.

The idea was to characterize the degradation of the polymer under different shear and elongational rates. For that, the ratio between the zero-shear viscosity after each injection and the initial zero-shear viscosity was used as a proxy of degradation, since the correlation between what is called the weight-average molecular weight

[8] For some of the experiments, it was possible to reinject the effluent until the 5th or 6th time. Although those results could not be use when comparing the degradation in between flow rates and capillaries, they can serve as additional informational on how the degradation occurs for subsequent injections.

and the zero-shear viscosity is well documented. (Kulicke & Kniewske, 1984) (Takahashi et al., 1985).

For the elongational flow in the capillaries, the average elongational rate may be calculated by:

$$\dot{\varepsilon} = \frac{d\varepsilon}{dt} = \frac{dv}{dx} = \frac{V - v}{d} = \frac{Q}{\pi d}\left(\frac{1}{r^2} - \frac{1}{R^2}\right)$$

Where Q is the flow rate, V is the velocity of the fluid in the constriction and v, in the straight portion of the capillary, d is the contraction length between the two radii, R is the entrance radius and r is the constriction radius, as depicted in

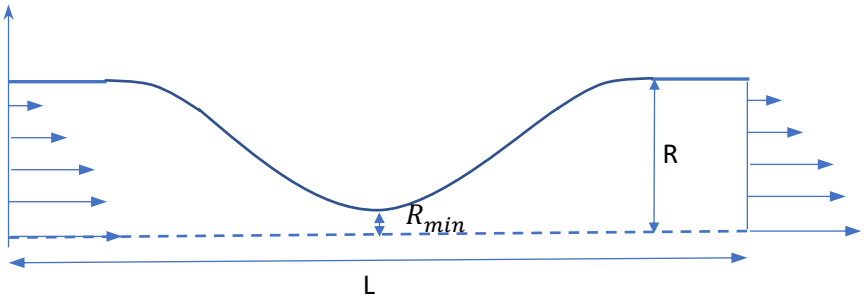

Figure 12.

The shear rate in the constriction was also calculated for each flow rate by the following equation:

$$\dot{\gamma} = \frac{4Q}{\pi r^3}$$

In order to estimate the imprecision or random error of the viscosity measurement and adjustment, a replication of the rheometer measurement and viscosity adjustment of a polymer sample was performed, and the standard deviation of the adjusted curves was obtained for each shear rate of the rheometer shear ramp. The maximum value of standard deviation for a specific shear rate obtained was 4% relatively to the average of the replicated viscosities.

3
Experimental results

3.1
Effluent viscosity curves

In **Figure 19** - *Viscosity curves for all effluents of the 0.07 cc/min flow rate* there are all the curves of the effluents that were injected through capillary 100:50 at the flow rate of 0.07 cc/min. The geometric forms represent the raw data from the rheometer and the continuous curve represent the Carreau model adjusted to the data for each injection. The original data refers to the effluent collected at the pump before flowing through the capillary (at 0.07 cc/min flow rate), which is the basis for comparison or the denominator of the viscosity ratios.

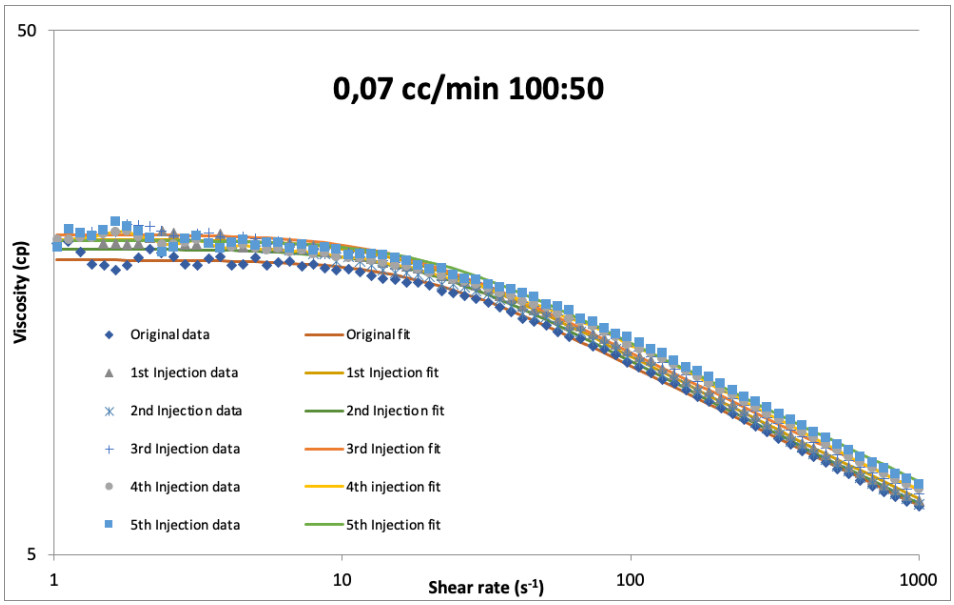

Figure 19 - Viscosity curves for all effluents of the 0.07 cc/min flow rate in capillary 100:50

In the image we can observe the scattering of the data at low shear rates mentioned in section 3.3.3.1. For this flow rate, the curves are close together and the variation of the viscosity is within 10% of that of the original data, as shown in Error! Reference source not found.

In **Figure 20** - *Viscosity curves for all effluents of the 0.1 cc/min flow rate in capillary* there are all the curves of the effluents that were injected through capillary 100:50 at the flow rate of 0.1 cc/min. The geometric forms represent the raw data from the rheometer and the continuous curve represent the Carreau model

adjusted to the data for each injection. The original data refers to the effluent collected at the pump before flowing through the capillary (at 0.1 cc/min flow rate). which is the basis for comparison or the denominator of the viscosity ratios.

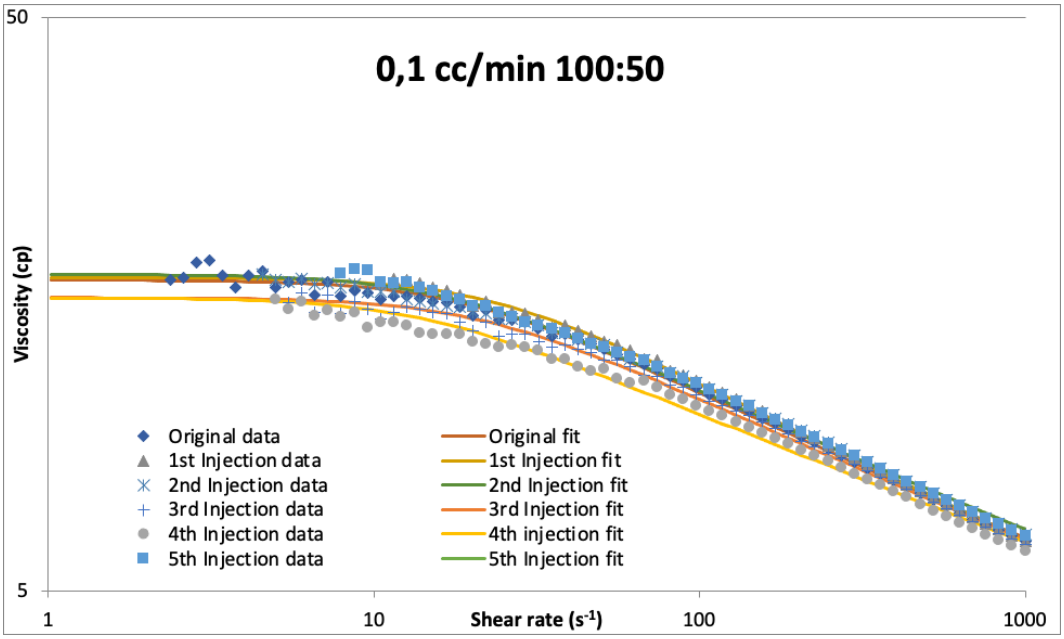

Figure 20 - Viscosity curves for all effluents of the 0.1 cc/min flow rate in capillary 100:50

In the image we can observe the scattering of the data at low shear rates mentioned in section 2.2.3.1. The outliers with excessive oscillation were not considered in the fitting into Carreau model and are not shown in the image. For this flow rate, the curves are close together and the variation of the viscosity is within 9% of that of the original data, as shown in **Table 6.**

In **Figure 21** there are all the curves of the effluents that were injected through capillary 100:50 at the flow rate of 0.2 cc/min. As in the previous graphs, the geometric forms represent the raw data from the rheometer and the continuous curve represent the Carreau model adjusted to the data for each injection. The original data refers to the effluent collected at the pump before flowing through the capillary (at 0.2 cc/min flow rate), which is the basis for comparison or the denominator of the viscosity ratios.

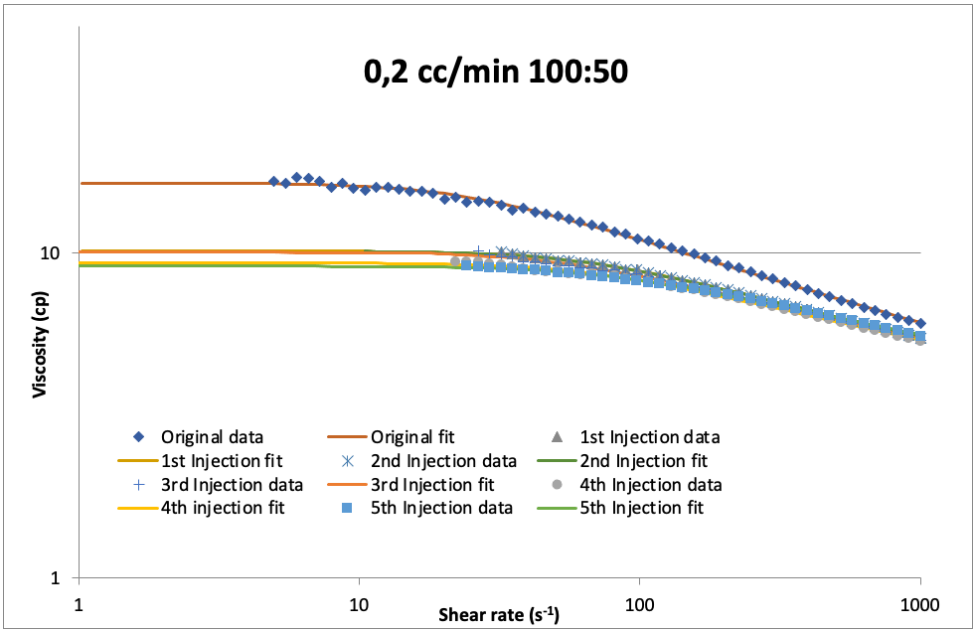

Figure 21 - Viscosity curves for all effluents of the 0.1 cc/min flow rate in capillary 100:50

Due to excessive oscillation at low shear rate, the initial points of viscosity were not considered in the fitting into Carreau model and are not shown in the image above. For some measurements, such as the ones in Figure 21, the curve was modeled mainly with data from higher shear rates (>10s^{-1}) and for that reason Section 3.1 presents the comparison of the viscosity ratios at higher shear rates (100 s^{-1} and 1000 s^{-1}).

One can observe in **Figure 21** a clear separation between the original effluent and the other effluents after injection and infer that degradation is taking place already in the first injection. Since the data of all the effluents, apart from the original data and fit, do not show variation higher than 10% between each other, the degradation for capillary 100:50 at 0.2 cc/min flow may be stabilizing already at the second injection.

Figure 22 brings all the curves of the effluents that were injected through capillary 100:50 at the flow rate of 0.5 cc/min. As in the previous graphs, the geometric forms represent the raw data from the rheometer and the continuous curve represent the Carreau model adjusted to the data for each injection. The original data refers to the effluent collected at the pump before flowing through the capillary (at 0.5 cc/min flow rate), which is the basis for comparison or the denominator of the viscosity ratios.

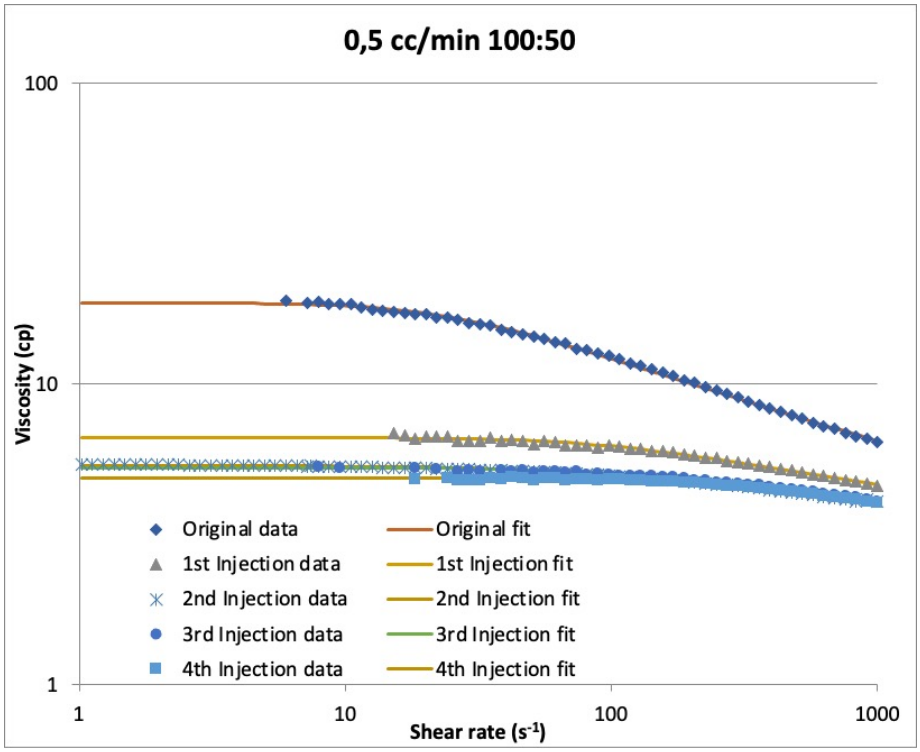

Figure 22 - Viscosity curves for all effluents of the 0.5 cc/min flow rate in capillary 100:50

The outliers with excessive oscillation were not considered in the Carreau model fit and are not shown in the image. One can observe a clear separation between the first five curves and infer that degradation is occurring for the first four injections. Only the 5th injection curve remains too close to the previous injection curve, which can be evidence for stabilization of degradation for the capillary 100:50 at 0.5cc/min at the 5th injection.

In **Figure 23** there are all the curves of the effluents that were injected through capillary 200:50 at the flow rate of 0.07 cc/min. As in the previous graphs, the geometric forms represent the raw data from the rheometer and the continuous curve represent the Carreau model adjusted to the data for each injection. The original data refers to the effluent collected at the pump before flowing through the capillary (at 0.07 cc/min flow rate), which is the basis for comparison or the denominator of the viscosity ratios.

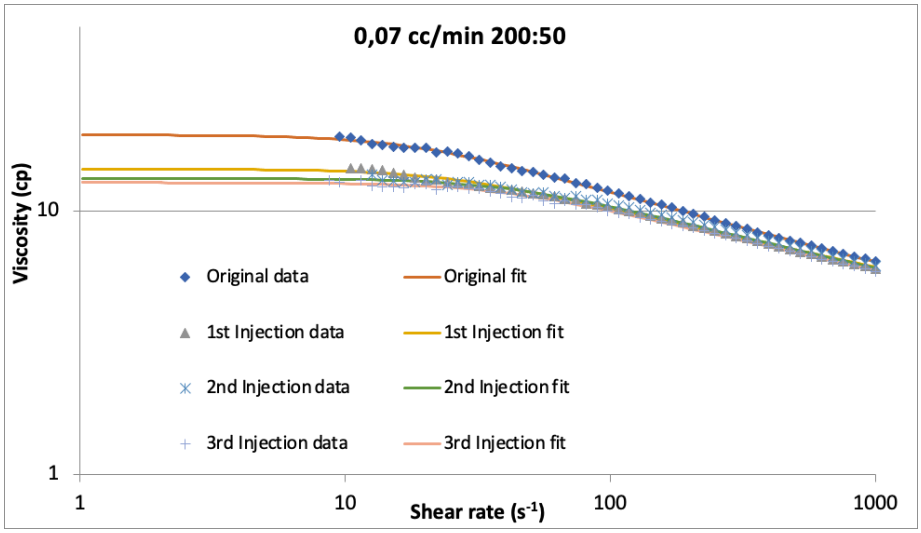

Figure 23 - Viscosity curves for all effluents of the 0.07 cc/min flow rate in capillary 200:50

The outliers with excessive oscillation were not considered in the Carreau model fit and are not shown in the image.

Differently than it is observed for capillary 100:50 at the same flow rate injection, the figure above depicts a clear separation between the original effluent and the other effluents after injection and one can infer that degradation is taking place already in the first injection. Since the data of all the effluents, apart from the original data and fit, do not show variation higher than 10% between each other, the degradation for capillary 200:50 at 0.07 cc/min flow may be stabilizing already at the second injection.

Figure 24 shows all the curves of the effluents that were injected through capillary 200:50 at the flow rate of 0.1 cc/min. As in the previous graphs, the geometric forms represent the raw data from the rheometer and the continuous curve represent the Carreau model adjusted to the data for each injection. The original data refers to the effluent collected at the pump before flowing through the capillary (at 0.1 cc/min flow rate), which is the basis for comparison or the denominator of the viscosity ratios.

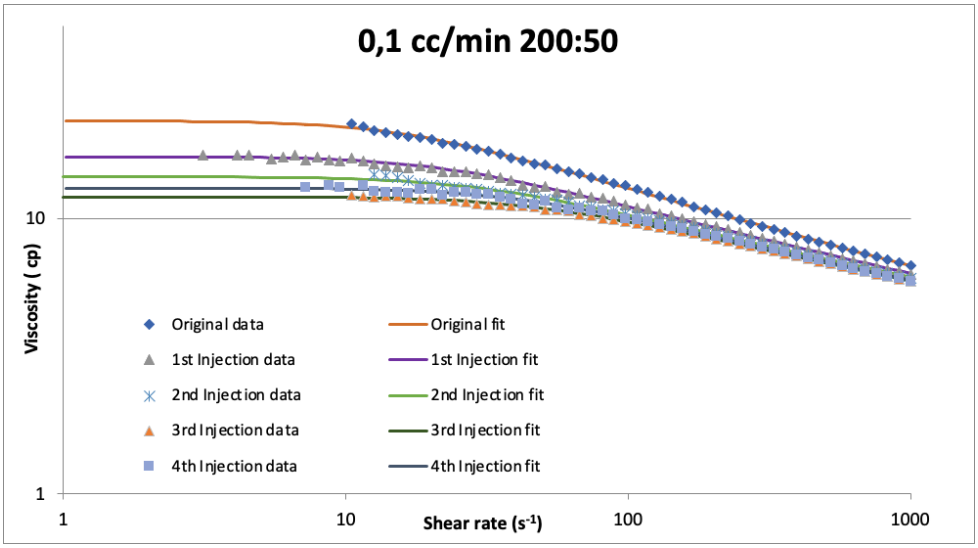

Figure 24 - Viscosity curves for all effluents of the 0.1 cc/min flow rate in capillary 200:50

The outliers with excessive oscillation were not considered in the Carreau model fit and are not shown in the image.

One can observe a clear separation between all the curves and infer that increasing degradation is taking place with each injection.

Figure 25 shows all the curves of the effluents that were injected through capillary 200:50 at the flow rate of 0.3 cc/min. As in the previous graphs, the geometric forms represent the raw data from the rheometer and the continuous curve represent the Carreau model adjusted to the data for each injection. The original data refers to the effluent collected at the pump before flowing through the capillary (at 0.3 cc/min flow rate), which is the basis for comparison or the denominator of the viscosity ratios.

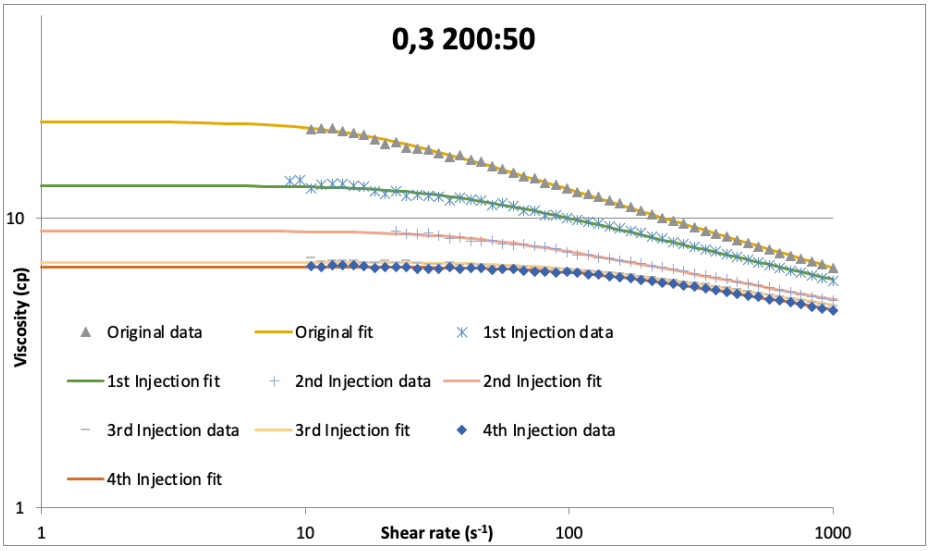

Figure 25 - Viscosity curves for all effluents of the 0.3 cc/min flow rate in capillary 200:50

The outliers with excessive oscillation were not considered in the Carreau model fit and are not shown in the image.

Similarly, to what happens for capillary 100:50 at 0.5 cc/min, one can observe a clear separation between the first five curves and infer that degradation is occurring for the first four injections. Only the 5th injection curve remains too close to the previous injection curve, which can be evidence for stabilization of degradation for the capillary 200:50 at 0.3 cc/min at the 5th injection.

Finally, **Figure 26** *Figure 19 - Viscosity curves for all effluents of the 0.07 cc/min flow rate*shows all the curves of the effluents that were injected through capillary 200:50 at the flow rate of 0.8 cc/min. As in the previous graphs, the geometric forms represent the raw data from the rheometer and the continuous curve represent the Carreau model adjusted to the data for each injection. The original data refers to the effluent collected at the pump before flowing through the capillary (at 0.8 cc/min flow rate), which is the basis for comparison or the denominator of the viscosity ratios.

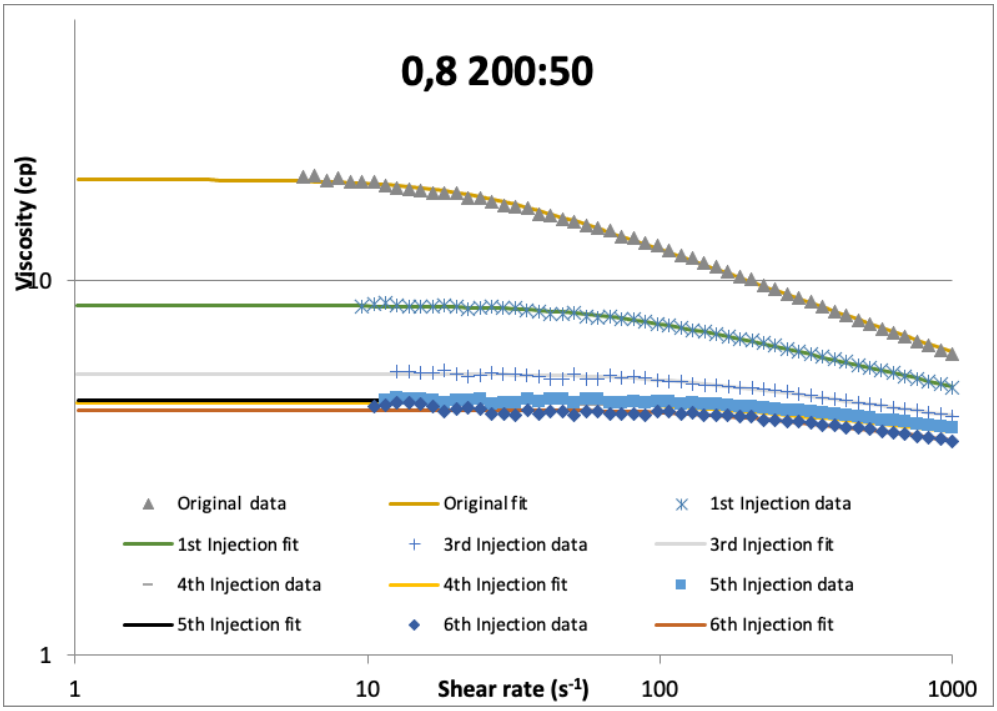

Figure 26 - Viscosity curves for all effluents of the 0.8 cc/min flow rate in capillary 200:50

Just as in the previous graphs, the outliers with excessive oscillation were not considered in the Carreau model fit and are not shown in the image.

One can observe a clear separation between the first four curves, and infer that incremental degradation is taking place until the 5th injection, when stabilization occurs for capillary 200:50 at 0.8 cc/min flow rate.

3.2
Analysis for each flow rate

3.2.1
Flow rate: 0.07 cc/min

For the first flow rate applied to both capillaries, we observe that there is degradation only in the effluent from capillary 200:50.

Table 1 - Results of degradation for 0.07 cc/min flow rate

Flow Rate (cc/min)					0.07				
capillary			200:50		capillary			100:50	
			$\eta_{100}/\eta_{100}{}^{o}$	$\eta_{1000}/\eta_{1000}{}^{o}$		$\eta_0/\eta_0{}^{o}$		$\eta_{100}/\eta_{100}{}^{o}$	

	$\eta_0/\eta_0{}^o$	η_{10} $/\eta_{10}{}^o$				η_{10} $/\eta_{10}{}^o$			η_{1000} $/\eta_{1000}{}^o$
1st	0.74	0.76	0.87	0.94	1st	1.1[9]	1.1	1.1	1.0
2nd	0.68	0.73	0.88	0.94	2nd	1.0	1.1	1.0	1.0
3rd	0.66	0.71	0.83	0.92	3rd	1.1	1.1	1.1	1.1
4th	N/A[10]	N/A	N/A	N/A	4th	1.1	1.1	1.1	1.1

Table 1 presents the degradation of the flow, represented by the ratio of the viscosities at a given shear rate of the original sample – that is, the sample of polymer that has just passed through the pump at 0.07 cc/min flow rate, before being injected through the capillary – and the respective viscosities of the effluents for each injection.

As explained in section 1.2.3, the Newtonian Plateau, represented by the zero-shear viscosity stems from the Carreau fit performed to the data obtained from the rheometer. Since there is a lot of uncertainty derived from the scattering of the data at low shear rates, we opted for also presenting the ratio of viscosities for different shear rates, utilizing the actual points of the rheometer curve and not the modelled curve.

From the data presented, it is safe to infer that there was no degradation of the polymer solution injected at capillary 100:50 at 0.07 cc/min. Whereas for capillary 200:50, the same flow rate was enough to cause a drop in the zero-shear viscosity as high as 34% (for the 4th injection).

One can also observe that, due to the shear-thinning of the viscosity curve, the degradation – for the capillary where it happened - becomes less expressive as higher the shear rate used as reference.

3.2.2
Flow rate: 0.1 cc/min

For the second flow rate applied to both capillaries, we observe that there is higher degradation, comparing to the 0.07 cc/min flow rate, in the effluent from capillary

[9] The values obtained that are higher than should be interpreted taking in consideration all the uncertainties of the rheology measurement and the fitting of the curve.
[10] For some flow rates, there are data missing, due to accidents during the experiments, such as capillary breakings, which were frequent during this study.

200:50, causing a drop in the zero-shear viscosity as high as 43% (for the 4th injection). The data is displayed in **Table 2.**

One can also notice a slight decline on the viscosity ratio for the effluents of capillary 100:50 after the 3rd injection. However, due to the uncertainties of the method, one cannot assure there was degradation yet.

Table 2 - Results of degradation for 0.1 cc/min flow rate

Flow Rate (cc/min)					0.1				
capillary			200:50		capillary			100:50	
	$\eta_0/\eta_0{}^o$	$\eta_{10}/\eta_{10}{}^o$	$\eta_{100}/\eta_{100}{}^o$	$\eta_{1000}/\eta_{1000}{}^o$		$\eta_0/\eta_0{}^o$	$\eta_{10}/\eta_{10}{}^o$	$\eta_{100}/\eta_{100}{}^o$	$\eta_{1000}/\eta_{1000}{}^o$
1st	0.74	0.75	0.85	0.93	1st	1.0	1.1	1.0	1.0
2nd	0.63	0.66	0.79	0.90	2nd	1.0	1.0	1.0	1.0
3rd	0.53	0.55	0.74	0.87	3rd	0.93	0.93	0.97	0.99
4th	0.57	0.62	0.76	0.88	4th	0.93	0.91	0.93	0.96

3.2.3
Flow rate: 0.3 cc/min (capillary 200:50) and 0.2 cc/min (capillary 100:50)

To optimize the range of elongational and shear rates of the study, different flow rates were used for each capillary from the third flow rate on. The results are displayed below, in **Table 3.**

Table 3 - Results of degradation for 0.3 and 0.2 cc/min flow rates

Flow Rate (cc/min)			0.3		Flow Rate (cc/min)			0.2	
capillary			200:50		capillary			100:50	
	$\eta_0/\eta_0{}^o$	$\eta_{10}/\eta_{10}{}^o$	$\eta_{100}/\eta_{100}{}^o$	$\eta_{1000}/\eta_{1000}{}^o$		$\eta_0/\eta_0{}^o$	$\eta_{10}/\eta_{10}{}^o$	$\eta_{100}/\eta_{100}{}^o$	$\eta_{1000}/\eta_{1000}{}^o$
1st	0.60	0.62	0.79	0.90	1st	0.62	N/A	0.80	0.90
2nd	0.42	N/A	0.60	0.77	2nd	0.62	0.65	0.79	0.90
3rd	0.33	0.36	0.53	0.74	3rd	0.61	N/A	0.78	0.89
4th	0.29	0.34	0.52	0.71	4th	0.57	0.66	0.73	0.88

Data from the flow at 0.3 cc/min through capillary 200:50 continues to display higher degradation with each injection number, reaching a 71% drop in zero-shear viscosity for the 4th injection.

When it comes to capillary 100:50, at 0.2 cc/min flow rate, double the previous rate, one can observe more significative decline in the viscosities ratio, enough to infer there is degradation from this rate on, reaching a 43% drop in zero-shear viscosity for the 4th injection.

3.2.4
Flow rate: 0.8 cc/min (capillary 200:50) and 0.5 cc/min (capillary 100:50)

The last two flow rates applied to capillary 200:50 and 100:50, respectively, were 0.8 cc/min and 0.5 cc/min. The results are displayed in **Table 4.**

Table 4 - Results of degradation for 0.8 and 0.5 cc/min flow rates

Flow Rate (cc/min)			0.8		Flow Rate (cc/min)			0.5	
capillary			200:50		capillary			100:50	
	$\eta_0/\eta_0{}^o$	$\eta_{10}/\eta_{10}{}^o$	$\eta_{100}/\eta_{100}{}^o$	$\eta_{1000}/\eta_{1000}{}^o$		$\eta_0/\eta_0{}^o$	$\eta_{10}/\eta_{10}{}^o$	$\eta_{100}/\eta_{100}{}^o$	$\eta_{1000}/\eta_{1000}{}^o$
1st	0.46	0.47	0.61	0.81	1st	0.36	0.39	0.50	0.72
2nd	N/A[11]	N/A	N/A	N/A	2nd	0.29	0.29	0.40	0.64
3rd	0.30	0.32	0.43	0.68	3rd	0.28	0.29	0.40	0.64
4th	0.25	0.30	0.37	0.62	4th	0.26	0.27	0.39	0.63

Data from the 0.8 cc/min flow rate through capillary 200:50 continues to display higher degradation with each injection number, reaching a 75% drop in zero-shear viscosity for the 4th injection.

The flow through capillary 100:50 shows similar levels of degradation, even though at a lower flow rate, 0.5 cc/min, which can indicate a stabilization on the level of degradation.

From the results discussed in sections 3.1.1 to 3.1.4, we observe that the degradation is set on lower flow rates for capillary 200:50. Even though both capillaries enable the same shear rate at the constriction – and there is a lower shear rate at the entrance and the exit of capillary 200:50 - the effluents of capillary 200:50 exhibit higher

[11] For some flow rates, there are data missing, due to accidents during the experiments, such as capillary breakings, which were frequent during this study.

levels of degradation, which can be initially attributed to the higher elongational rates observed in the flow though capillary 200:50.

3.3
Analysis by number of injections

Figure 27 and **Figure 28** illustrate the zero-shear viscosity ratios for the first injections of each flow rate plotted as a function of the calculated elongational rate and shear rate, respectively. Both graphs show that for low values of extensional and shear rate, only capillary 200:50 effluents show degradation.

At this point, it is important to have in mind that the values of extensional and shear rates presented were calculated as shown in section 2.4, which means they represent the average extensional rate between the two radii of each capillary and the maximum shear rate, at the constriction of the capillary, and as such do not represent the history of shear and elongational rates for each capillary. Moreover, both rate formulas can also be described as $K.Q$, where K is a constant for each capillary and Q is the flow rate, which means that a similar curve shape is expected for both types of deformation.

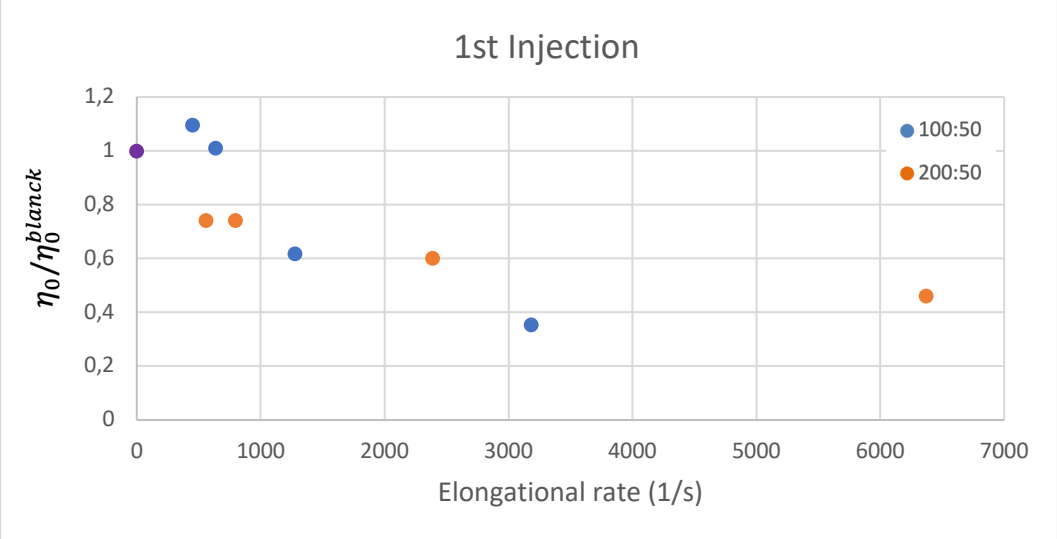

Figure 27 - Degradation based on the zero-shear viscosity in function of the elongational rate for the first injections of each flow rate.

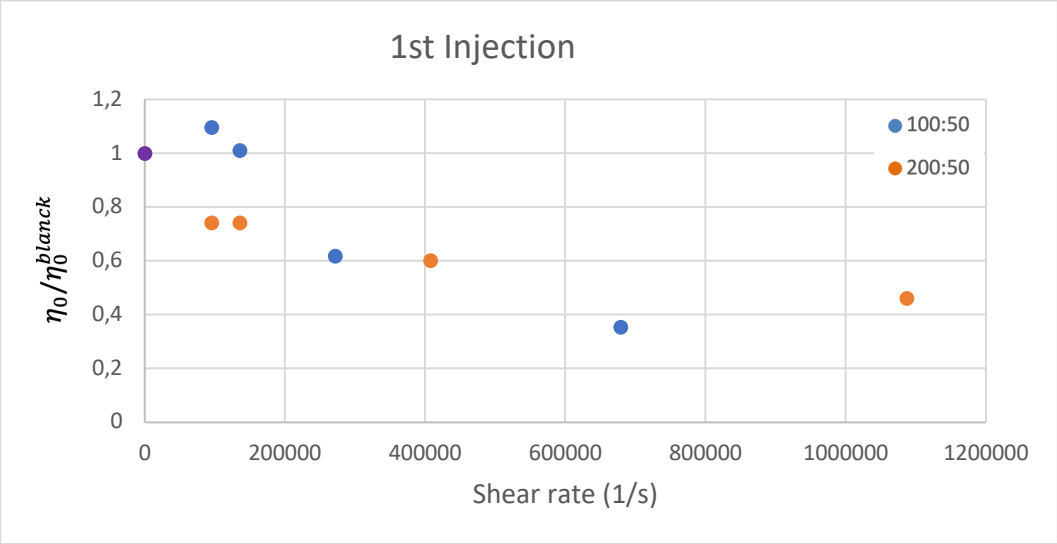

Figure 28 - Degradation based on the zero-shear viscosity in function of the shear rate for the first injections of each flow rate.

For the first injections, the lowest viscosity ratio obtained is 0.36, at the elongational rate of ≈3,000 s^{-1} and respective shear rate of ≈600,000 s^{-1}.

Figure 29 and **Figure 30** illustrate the zero-shear viscosity ratios for the second injections of each flow rate plotted as a function of the calculated elongational rate and shear rate, respectively. We still observe that for the two lowest values of extensional and shear rate, only capillary 200:50 effluents show degradation.

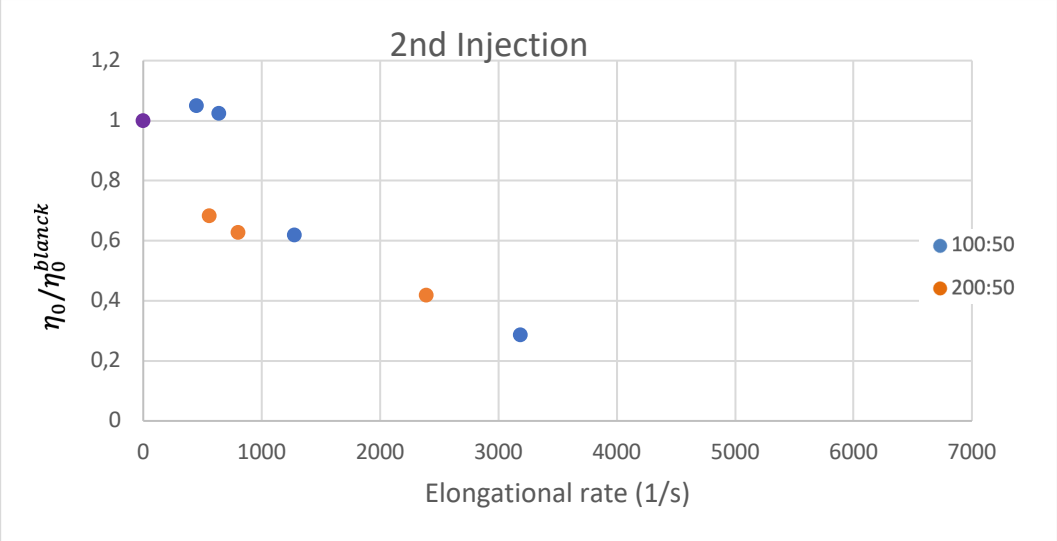

Figure 29 - Degradation based on the zero-shear viscosity in function of the elongational rate for the second injections

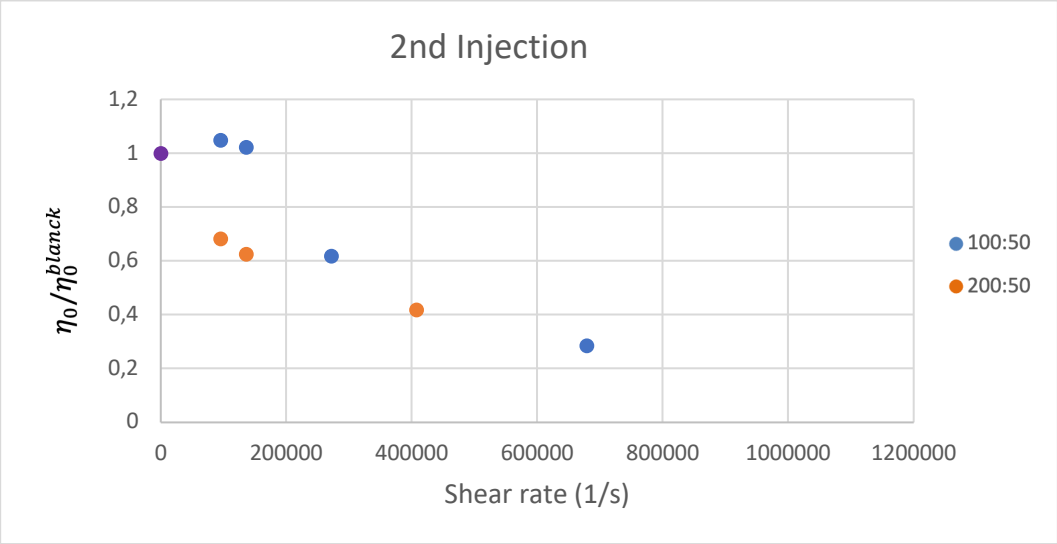

Figure 30 - Degradation based on the zero-shear viscosity in function of the shear rate for the second injections

Moreover, for rates above the critical rate for degradation of each capillary, the second injections are able to break the polymer even more, as expected. The lowest viscosity ratio obtained is 0.29, 19% lower than that obtained at the first injections.

Figure 31 and **Figure 32** illustrate the zero-shear viscosity ratios for the third injections of each flow rate plotted in function of the calculated elongational rate and shear rate, respectively.

For the lowest flow rate studied, which corresponds to 446 s^{-1} elongational rate and 95069 s^{-1} shear rate, we can still affirm there is no degradation of the polymer solution, event at the third injection. However, for the second lowest flow rate, from the third injection on – as we will discuss further – there is a viscosity ratio below 1. Although that would mean there is degradation taking place, the deviation of the ratio (1-0.93 = 0.07), is still too little not be mistaken for the uncertainties of the method.

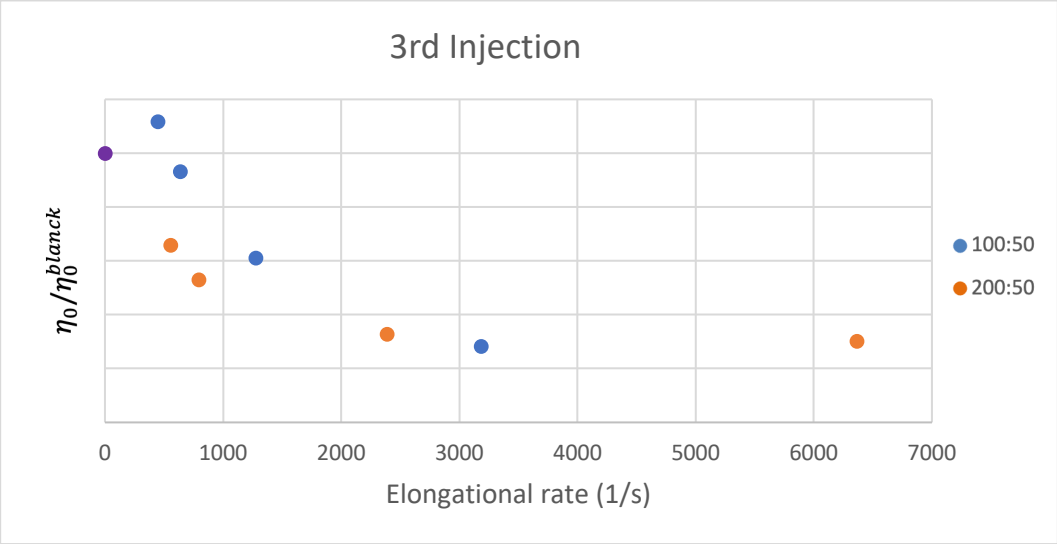

Figure 31 - Degradation based on the zero-shear viscosity in function of the elongational rate for the third injections

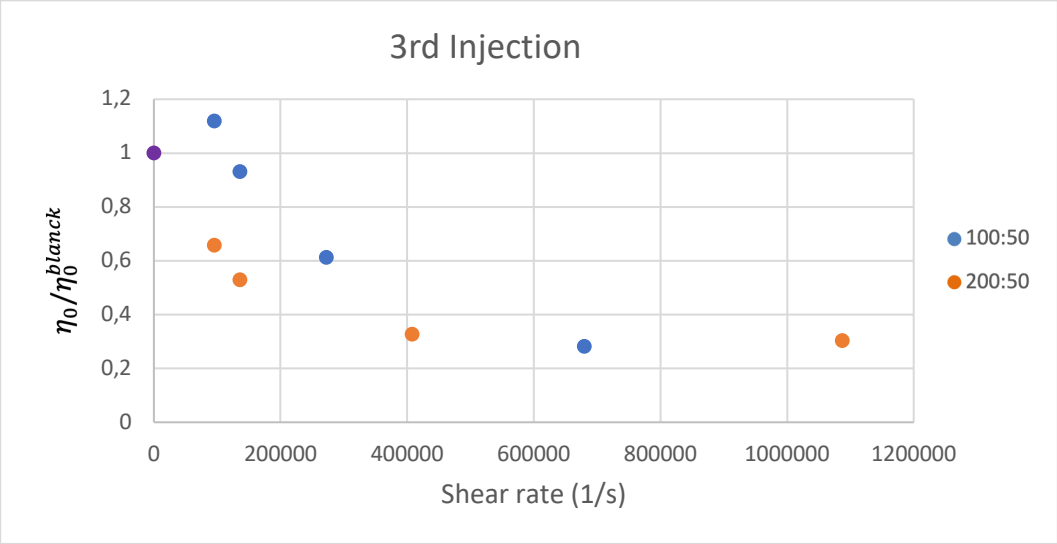

Figure 32 - Degradation based on the zero-shear viscosity in function of the shear rate for the third injections

The lowest viscosity ratio obtained is 0.28, 21% lower than that obtained at the first injections and 1.4%, at the second injections. Such low variation (1.4%) may be attributed to the uncertainties of the method and in fact, the polymer solution might be reaching a degradation plateau from the third injection on at the highest shear rates.

Figure 31 and **Figure 34** illustrate the zero-shear viscosity ratios for the fourth injections of each flow rate plotted in function of the calculated elongational rate and shear rate, respectively.

For the lowest flow rate studied, which corresponds to 446 s^{-1} elongational rate and the 95069 s^{-1} shear rate, we can still affirm there is no degradation of the polymer solution, even after the fourth injection. However, for the second lowest flow rate, from the third injection on there is a viscosity ratio below 1. As discussed for the third injection case, although that would mean there is degradation taking place, the deviation of the ratio (1-0.93 = 0.07), is still too little not be mistaken with the uncertainties of the method.

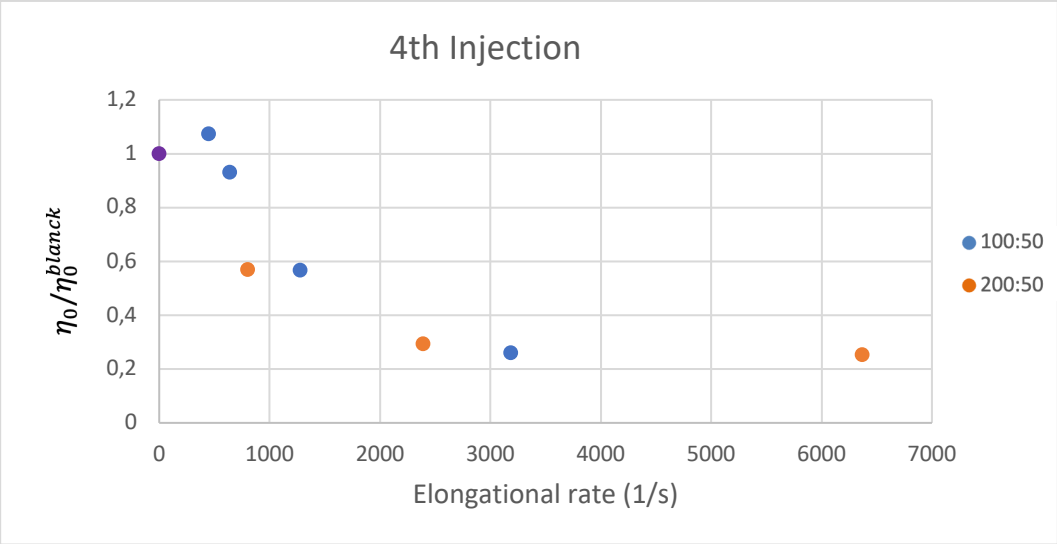

Figure 33 - Degradation based on the zero-shear viscosity in function of the elongational rate for the fourth injections

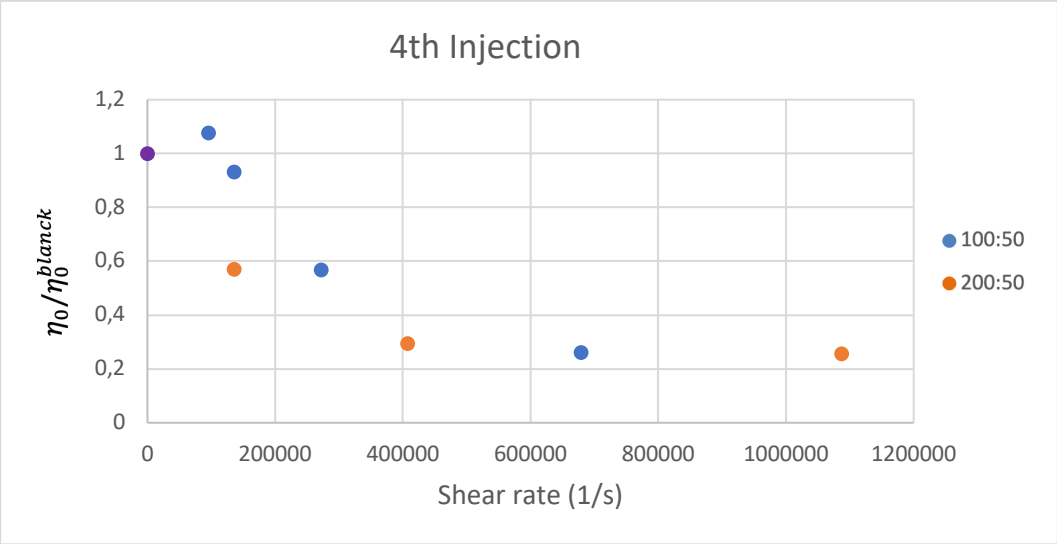

Figure 34 - Degradation based on the zero-shear viscosity in function of the shear rate for the fourth injections

When comparing the graphs that showed degradation data, especially **Figures 31** to **34**, one can observe that those presented as a function of $\dot{\varepsilon}$ show a more cohesive behavior, regardless of whether they were obtained from capillary 200:50 or 100:50, than those of $\dot{\gamma}$, which can indicate that mechanical degradation occurs mostly due to extensional deformation, rather than shear rate.

The lowest viscosity ratio obtained is 0.25, for the elongational rate of 6366 s^{-1}, 46% lower than that obtained at the first injections at the same rate and 15%, at the third injections. However, for the other graphs, the lowest ratio was obtained at the elongational rate of 3183 s^{-1} and if we compare the lowest ratio of the fourth injection with that of the previous injections, we get a decrease of 31%, in comparison with the first injection and 2.3%, with the third.

As expected, the highest variations of the viscosity ratio for each flow rate happened at the first injections. **Table 5** below shows the incremental degradation of the polymer solution for each additional injection, calculated by:

$$ID = \frac{\eta_{0i}}{\eta_{0(blanck)}} - 1$$

Where ID is the incremental degradation, η_{0i} is the zero-shear viscosity for the effluent of the i^{th} injection and $\eta_{0(blanck)}$ is the original η_0, from the effluent collected at the pump before flowing through the capillary.

Table 5 - Incremental degradation of the polymer for each additional injection

Cap	flow rate (cc/min)	1st	2nd	3rd	4th
100:50	0.07	-[12]	-	-	-
	0.10	-	-	-7%	-7%
	0.20	-38%	-38%	-39%	-43%
	0.50	-64%	-71%	-72%	-74%
200:50	0.07	-26%	-32%	-34%	
	0.10	-26%	-37%	-47%	-43%
	0.30	-40%	-58%	-67%	-71%
	0.8	-54%		-70%	-75%

[12] The table only presents data where degradation was observed, ID <0.

Table 6 - Experiment results

Flow Rate (cc/min)	Cap	$\dot{\gamma}$ (s-1)	$\dot{\varepsilon}$ (s-1)	$\eta_0{}^{branco}$ (cp)	$\eta_0/\eta_0{}^{branco}$			
					1st	2nd	3rd	4th
0.07	100:50	95069	446	18.2	1.1	1.0	1.1	1.1
0.1	100:50	135812	637	17.4	1.0	1.0	0.93	0.93
0.2	100:50	271624	1273	16.5	0.62	0.62	0.61	0.57
0.5	100:50	679061	3183	18.6	0.36	0.29	0.28	0.26
0.07	200:50	95069	557	19.5	0.74	0.68	0.66	N/A
0.1	200:50	135812	796	22.6	0.74	0.63	0.53	0.57
0.3	200:50	407437	2387	21.5	0.60	0.42	0.33	0.29
0.8	200:50	1086498	6366	18.6	0.46	N/A	0.30	0.25

4
Conclusion

Experiments were conducted to study the degradation of a semi diluted (2000 ppm) aqueous solution of PEO, using two capillaries with different entrance diameter (100 μm and 200 μm) both with 50 μm diameter constriction, creating Fast-Transient Flows in their center. The geometry represents a model of a pore throat in a porous media. The different geometries allowed flows at a fixed flow rate to have the same maximum shear rate and different extensional rate. Different injection rates were imposed in order to observe different shear and extensional rates in the system. The effluent of the flow was collected, and reinjected, and rheological properties of the fluids were used as proxies for the degradation of the solution.

From the data presented, we observe that for the more abrupt contraction (200:50), the minimum flow rate needed for degrading the polymer solution is lower than that needed for the 100:50 contraction. This result, when analyzed purely under shear rate perspective, is not reasonable, since the shear rates to which the polymer is subjected at capillary 200:50 are equal or lower than those of capillary 100:50. Therefore, it is possible to infer that the abruptness of the contraction plays a role in the degradation, which means elongational rate may be responsible for the lower critical flow rate.

Moreover, when comparing the graphs that showed degradation data, one can observe that those presented as a function of $\dot{\varepsilon}$ show a more cohesive behavior than those of $\dot{\gamma}$, which can indicate that mechanical degradation occurs mostly due to extensional deformation, rather than shear rate.

It is also observed a pattern for how the degradation occurs with subsequent injections. Increasing the flow rate above its critical value, considerable incremental degradation is observed with each additional injection.

This way, one can infer that subsequent injections cause incremental degradation before approaching a stabilization plateau and that higher flow rates generated lower degradation plateaus. The very degradation plateau value in function of shear rate is also expected to stabilize at higher flow rates, as there is a clear limit for breaking the polymer chain. Nonetheless, this work has not investigated enough flow rates to be able to observe that behavior.

As suggestions for research on this topic, there is (i) further investigation with different capillaries and flow rates, so as to explore the critical flow rate and the stabilization plateau for various capillaries, including those without any constriction – generating a simple shear flow and (ii) the use of Gel Permeation Chromatography – GPC to characterize the polymer solutions. Although the use of rheometers is common for laboratory characterization of IOR fluids, there are several limitations related to the use of rheology properties as proxies for degradation, as described in this study.

5
References

AL-SHAKRY, B. et al. Impact of Mechanical Degradation on Polymer Injectivity in Porous Media. **Polymers**, [s. L.], v. 10, n. 742, 2018.

BARNES, H. A. **A Handbook of Elementary Rheology**. Institute of Non-Newtonian Fluid Mechanics University of Wales, p. 151-164, 2000.

BENTLEY, B.; LEAL, L. A computer-controlled four-roll mill for investigations of particle and drop dynamics in two-dimensional linear shear flows. **Journal of Fluid Mechanics**, [s. L.], v. 167, p. 219-240, 1986.

BORCHARDT, J. K. Chemicals Used in Oil-Field Operations. In:_____. **Oil-Field Chemistry**. [s. L.]: ACS Symposium Series, 1989. p. 3-54.

CHANDRA, B.; SHANKAR, V.; DAS, D., Onset of transition in the flow of polymer solutions through microtubes. **Journal of Fluid Mechanics**, [s. L.], v. 844, p. 1052-1083, 2018.

DAUBEN, D. L.; MENZIE, D. E. Flow of Polymer Solutions Through Porous Media. **Journal of Petroleum Technology**, [s. L.], v. 19, n. 8, p. 1065–1073, 1967.

DELSHAD, M. et al. Mechanistic Interpretation and Utilization of Viscoelastic Behavior of Polymer Solutions for Improved Polymer-Flood Efficiency. In: SPE/DOE Improved Oil Recovery Symposium, 2008, Tulsa. **Paper.** Tulsa: SPE, 2008. ISBN: 978-1-55563-225-0.

DEVANAND, K.; SELSER, J. Polyethylene oxide does not necessarily aggregate in water. **Nature**, [s. L.], v. 343, p. 739–741, 1990.

DIJKSTRA, D. et al. Guidelines for checking performance and verifying accuracy of rotational rheometers: Viscosity measurements in steady and oscillatory shear (IUPAC Technical Report). **Pure and Applied Chemistry**, [s. L.], v. 86, n. 12, 2014.

DONG, H. et al. Review of Practical Experience & Management by Polymer Flooding at Daqing. **SPE Journal**, USA, apr. 2008. ISBN: 978-1-55563-225-0.

DUPAS, A. et al. Mechanical Degradation Onset of Polyethylene Oxide Used as a Hydrosoluble Model Polymer for Enhanced Oil Recovery. **Oil & Gas Science and Technology Journal**, [s. L.], v. 67, p. 931-940, 2012.

EWOLDT, R.; CARETTA, M. J. A. L. Experimental challenges of shear rheology: how to avoid bad data. In: EWOLDT, R. et al. Complex Fluids in Biological Systems. [s. L.]: Springer, 2015. p. 207-241.

FRANK, F.; KELLER, A.; MACKLEY, M. Polymer chain extension produced by impinging jets and its effect on polyethylene solution. **Polymer**, [s. L.], v. 12, n. 7, p. 467-473, 1971.

JENNINGS, R. R. et al. Factors Influencing Mobility Control By Polymer Solutions. Journal of Petroleum Technology. **Journal of Petroleum Technology**, [s. L.], v. 23, v. 3, p. 391–401, 1971.

JOHNSTON, M. T. & EWOLDT, R. H., Precision rheometry: Surface tension effects on low-torque measurements in rotational rheometers. **Journal of Rheology**, [s. L.], v. 57, issue 6, 2013.

JOUENNE, S.; CHAKIBI, H.; LEVITT, D. Polymer Stability After Successive Mechanical-Degradation Events. **SPE Journal**, [s. L.], v. 23, n. 1, p. 18-33, 2018.

KELLER, A.; ODELL, J. The extensibility of macromolecules in solution; a new focus for macromolecular science. **Colloid & Polymer Science**, [s. L.], issue 263, p. 181-201, 1985.

KULICKE, W.; KNIEWSKE, R. The shearviscosity dependenceon concentration, molecular weight, and shear rate of polystyrene solutions. **Rheologica Acta**, [s. L.], v. 23, 1984.

LIMA, N. M. D. **Análise do Deslocamento de Óleo por Soluções Poliméricas em Microescala**. 2015. 80 f. Dissertação (mestrado) – Pontifícia Universidade Católica do Rio de Janeiro, Rio de Janeiro, 2015.

MILES, M.; KELLER, A. Conformational relaxation time in polymer solutions by elongational flow experiments: 2. Preliminaries of further developments: chain retraction; identification of molecular weight fractions in a mixture. **Polymer**, [s. L.], v. 21, p. 1295-1298, 1980.

NGHE, P.; TABELING, P.; AJDARIB, A. Flow-induced polymer degradation probed by a high throughput microfluidic set-up. **Journal of Non-Newtonian Fluid Mechanics**, [s. L.], v. 165, p. 313-322, 2010.

NGUYEN, T.; KAUSCH, H.-H. **Flexible Polymer Chains in Elongational Flow**: Theory and Experiment. [s. L.]: Springer-Verlag Berlin Heidelberg, 1999.

PINHO, F. et al. Transport Phenomena Research Center (CEFT): Research complex flows of complex fluids. In: JAPAN-PORTUGAL NANO-BIOMEDICAL ENGINEERING SYMPOSIUM, 2011, United Kingdom. **Paper**… United Kingdom: BME, 2011.

RABIN, Y. On the mechanism of stretching and breaking of polymers in elongational flows. **Journal of Non-Newtonian Fluid Mechanics**, [s. L.], v. 30, p. 119-123, 1988.

RAMSEY, S. M. **Practical Wellbore Hydraulics and Hole Cleaning**. [s. L.]: Gulf Professional Publishing, 2019.

RYSKIN, G. Calculation of the effect of polymer additive in a converging flow. **Jounal of Fluid Mechanics**, [s. L.], v. 178, p. 423-440, 1987.

SERIGHT, R. et al. New Insights into Polymer Rheology in Porous Media. **SPE Jornal**, Tulsa, v. 16 n. 1, p. 35-42, 2010.

SERIGHT, R. S. How Much Polymer Should Be Injected During a Polymer Flood? Review of Previous and Current Practices. **SPE Journal**, [s. L.], v. 22, n. 1, 2017.

SERIGHT, R. S. The Effects of Mechanical Degradation and Viscoelastic Behavior on Injectivity of Polyacrylamide Solutions. **Society of Petroleum Engineers Journal**, [s. L.], v. 23, n. 3, p. 475-485, 1983.

SKAUGE, A. et al. Polymer Flow in Porous Media: Relevance to Enhanced Oil Recovery. **Colloids Interfaces**, [s. L.], v. 2, n. 3, p. 27, 2018.

SMITH, F. W. The Behavior of Partially Hydrolyzed Polyacrylamide Solutions in Porous Media. **Journal of Petroleum Technology**, [s. L.], v. 22, n. 2, p. 148-156, 1970.

SORBIE, K. S. **Polymer-Improved Oil Recovery**. Boca Raton: CRC Press, 2000.

SPEIGHT, J. G. Nonthermal Methods of Recovery. In:_____. **Heavy Oil Recovery and Upgrading**. [s. L.]: Gulf Professional Publishing, 2019. p. 49-11.

STAVLAND, A. et al. Polymer Flooding - Flow Properties in Porous Media versus Rheological Parameters. **SPE Journal**, Spain, p. xx-xx, jun. 2010. ISBN: 978-1-61399-428-3.

SUNTHAR, P. Polymer rheology. In: DESHPANDE, A. P.; KRISHNAN, J. M.; KUMAR, S. (Eds.). **Rheology of complex fluids**. New York: Springer, 2010. p. 171-191.

TAKAHASHI, Y. et al. Zero-Shear Viscosity of Linear Polymer Solutions over a Wide Range of Concentration. **Macromolecules**, [s. L.], v. 18, n. 5, p. 1002-1008, 1985.

VAN DEN ENDE, T. **Extensional viscosity aspects of HPAM in porous flow**: An experimental and numerical study. Netherlands: Delft University of Technology, 2015. MSc Thesis.